7-17-2013 12:00 AM

Somatosensory stimulation modulates heart rate variability changes induced by isometric handgrip exercise

Jacquie Baker
The University of Western Ontario

Supervisor
Dr. Kevin Shoemaker
The University of Western Ontario

Graduate Program in Kinesiology
A thesis submitted in partial fulfillment of the requirements for the degree in Master of Science

SOMATOSENSORY STIMULATION MODULATES HEART RATE VARIABILITY CHANGES INDUCED BY ISOMETRIC HANDGRIP EXERCISE

(Thesis format: Monograph)

by

Jacquie Baker

Graduate Program in Kinesiology

A thesis submitted in partial fulfillment
of the requirements for the degree of
Master of Science in Integrative Physiology

The School of Graduate and Postdoctoral Studies
The University of Western Ontario
London, Ontario, Canada

ABSTRACT

Functional imaging reveals overlapping forebrain and basal ganglia regions associated with heart rate (HR) and heart rate variability (HRV) regulation. Somatosensory stimulation (STIM) and isometric handgrip (HG) were used to test the hypotheses that a) STIM would modulate HG-induced changes to HR and HRV, and b) HG+STIM would produce different cortical activation relative to HG alone (n=12). During STIM, high-frequency (HF)-HRV increased ($p<0.05$), whereas HR did not change. During HG, HF-HRV decreased ($p<0.01$) while HR increased ($p<0.001$). HG+STIM reversed the HG-induced change in HF-HRV ($p<0.01$). However, the HR response to HG remained unaffected. HG increased insular activation, while ventral medial prefrontal cortex (vMPFC) activity decreased. HG+STIM produced similar vMPFC deactivation. However, insular activation was no longer evident. These data indicate that somatosensory inputs through STIM can modulate HG-induced changes to HF-HRV. Different insular activations during HG versus HG+STIM suggest afferent signals to the insula may inhibit descending motor signals affecting HF-HRV.

KEY WORDS: somatosensory stimulation, handgrip exercise, heart rate variability, heart rate, insula cortex, ventral medial prefrontal cortex, functional MRI.

ACKNOWLEDGEMENTS

When I started on this path, I was told, “By the time you are done your Masters, you will be ready to do your Masters”. Now that I am done, I can respect how true that statement is. I have gained so much knowledge and hands-on experience throughout the completion of this dissertation. However, it would not have been possible without the help of so many people in so many ways.

To Dr. Kevin Shoemaker. Who you are as a person, an educator and a scientist, is something I aspire to in my future. You have my deepest appreciate for all your time and continued efforts in the past two years. Your intelligence, dedication, and passion for science are next to none, and I could not have imagined working with anyone else.

To my advisory and defense committees: Dr. Matthew Heath, Dr. Glen Belfry, and Dr. Ruth Martin. Thank you for your comments and contributions throughout the completion of this dissertation and degree.

To Dr. Liza Stathokostas. Over the years you have gone above and beyond what would be expected of any professor. Your encouragement, support, and of course, words of wisdom, have kept me on track on countless occasions.

The unwavering support of family and friends has given me the foundation for success, and this accomplishment is a testament to that. To Mom, Frank, Mary, and Kurt, you are my biggest fans, and this dissertation would not be what it is without you. Perhaps, when you read it you will finally know what I have been talking about for the last two years. With that said, thank you for your support, love and patience through this journey.

This dissertation would certainly not be possible without the continued contributions of past and present lab mates. Thank you everyone for your continued

efforts through participation (on multiple occasions), data collection, analysis, and overall completion of this work. More importantly, you have made my time in the lab an enjoyable one, and I hope the friendships we have established here continue as we move toward, and are successful in the next steps of our careers. Special thanks go out to Dr. Sophie Lalande and Katelyn Norton. Katelyn, I could not have completed this study without your assistance both at the MRI and throughout the entire brain imaging analysis. Sophie, I cannot thank you enough for your assistance and general enthusiasm in the lab, and for your continued efforts throughout the entire process of this dissertation.

Nicki, Thank you, from the bottom of my heart, for just being you. During good times, stressful times, and crunch times, you have been there. When I consider where we came from, to where we are now, I am in awe of what we have created. Everyday with you is better than the last, and for that reason, I look forward to each and every tomorrow, and wherever tomorrow may takes us.

In writing this, I have found it difficult to truly express my gratitude to everyone who has been a part of this accomplishment. However, I hope my many thanks will resound with all of you. For that reason, I dedicate this to you.

TABLE OF CONTENTS

LIST OF TABLES

LIST OF FIGURES

LIST OF APPENDICES

LIST OF ABBREVIATIONS

ACC	Anterior Cingulate Cortex
ACH	Acetylcholine
ANOVA	Analysis of Variance
ANS	Autonomic Nervous System
B^0	Main Magnetic Field
B^1	Additional Magnetic Field
BOLD	Bold-Oxygen-Level-Dependent
BP	Blood Pressure
BRS	Baroreflex Sensitivity
CAN	Cortical Autonomic Network
CHF	Chronic Heart Failure
CNS	Central Nervous System
dACC	Dorsal Anterior Cingulate Cortex
dHb	Deoxyhemoglobin
ECG	Electrocardiography
EMLA	Eutectic Mixture of Local Anesthetic
EPI	Echo Planar Imaging
FDR	False Discovery Rate
fMRI	Functional Magnetic Resonance Imaging
GLM	General Linear Model
H	Hydrogen
Hb	Hemoglobin
HF-HRV	High-Frequency Heart rate Variability
HG	Handgrip
HR	Heart Rate
HRR	Heart Rate Recovery
HRV	Heart Rate Variability
IML	Intermediolateral
LBNP	Lower Body Negative Pressure
LF	Low Frequency
M1	Primary Motor Cortex
MAP	Mean Arterial Pressure
MCC	Mid Cingulate Cortex
MRI	Magnetic Resonance Imaging
MSNA	Muscle Sympathetic Nerve Activity
MVC	Maximal Voluntary Contraction
NE	Norepinephrine
NN	Normal-Normal Interval
PCC	Posterior Cingulate cortex
PNS	Parasympathetic Nervous System
RHR	Resting Heart Rate

RR INT	R-R Interval
SI	Primary Somatosensory Cortex
SII	Secondary Somatosensory Cortex
SDNN	Standard Deviation of the Normal-Normal Interval
SMA	Supplementary Motor Area
SNS	Sympathetic Nervous System
SSNS	Somatosensory Electrical Nerve Stimulation
TE	Echo Time
TR	Time to Repetition
STIM	Somatosensory Stimulation
VLF	Very Low Frequency
vMPFC	Ventral Medial Prefrontal Cortex

CHAPTER 1 – INTRODUCTION

The autonomic nervous system is in a perpetual state of change in order to maintain balance between its two main neural divisions, the parasympathetic (vagal), and the sympathetic branch. Each neural division fluctuates to support internal homeostasis. Heart rate variability (HRV) is a common measurement used to evaluate autonomic modulations of the heart through the main neural branches at the sinoatrial node.

Heart rate variability can be defined as the degree of fluctuation around the mean heart rate (HR) (van Ravenswaaij-Arts, Kollee, Hopman, Stoelinga, & van Geijn, 1993). It is currently believed that these beat-to-beat fluctuations reflect a dynamic response of cardiovascular control systems to various physiological perturbations. High HRV demonstrated more frequent spontaneous fluctuations of HR, and a more complex interplay between the neural divisions (Pagani, et al., 1986). The high frequency domain (HF) (0.15-0.4Hz) of HRV is primarily reflective of vagal activity (Malik, et al., 1996) (Pagani, et al., 1986; Pomeranz, et al., 1985), unlike the low (0.04-0.15Hz) and very low frequency (0.0033-0.04Hz) (van Ravenswaaij-Arts, Kollee, Hopman, Stoelinga, & van Geijn, 1993).

Cardiovascular responses to voluntary muscular contraction such as isometric handgrip (HG) exercise often include a decrease in HRV (Hollman & Morgan, 1997), in addition to increases in HR, blood pressure (BP), cardiac output (Lind, Taylor, Humphreys, Kennelly, & Donald, 1964) and, at higher intensities, muscle sympathetic nerve activity (Maciel, Gallo Jr., JA, & Martins, 1987). In contrast,

somatosensory stimulation of muscle sensory nerve afferents has been shown to increase HRV in the HF domain (Goswami, Frances, & Shoemaker, 2010), and reduce sympathetic activity via sympatho-inhibition (Hollman and Morgan, 1997; Jacobsson, et al. 2000; Owens, Atkinson and Lees, 1979).

There are four types of muscle sensory nerve afferents, namely types I, II, III, and IV, that can detect and transmit afferent information back to the brain to affect autonomic cardiovascular control. Type III and IV are functionally involved in cardiovascular arousal reflexes during fatiguing contractions (McCloskey and Mitchell 1972). However, less is known about the role of Type I and II muscle afferents in cardiovascular control. Recent advances in functional imaging now provide a powerful tool for addressing such questions. Functional imaging studies during painful and non-painful stimulation have identified muscle afferent representation within the cortical autonomic network (Arienzo, et al., 2006; Goswami, Frances, & Shoemaker, 2010). However, their role in autonomic cardiovascular control has not fully been elucidated.

The cortical autonomic network (CAN) has been exposed by clinical and neuroimaging studies as a network of forebrain regions associated with autonomic control. The ventral medial prefrontal cortex (vMPFC), the anterior cingulate cortex (ACC), and the insular cortex are some key cortical structures that make up the CAN (Verberne & Owens, 1998; Kimmerly, O'Leary, Menon, Gati, & Shoemaker, 2005; Wong, Masse, Kimmerly, Menon, & Shoemaker, 2007b). Each structure projects directly or indirectly to subcortical structures that modulate autonomic responses, making each of them instrumental in autonomic control (Verberne & Owens, 1998).

The vMPFC, ACC and insula have all been implicated in HR and HRV during both effortful tasks (King, Menon, Hachinski, & Cechetto, 1999; Critchley, et al., 2003; Wong, Masse, Kimmerly, Menon, & Shoemaker, 2007b; Goswami, Frances, & Shoemaker, 2010) and somatosensory stimulation of muscle afferents (Coghill, et al., 1994; Arienzo, et al., 2006; Goswami, Frances, & Shoemaker, 2010). However, despite these shared regions of HR and HRV regulation, little is known about the cortical autonomic modulation when both tasks are combined. Hollman & Morgan (1997) performed HG with concurrent stimulation, and found stimulation reduced the HG-mediated sympathetic and BP responses. The authors suggested that stimulation of Type I and II afferents resulted in sympatho-inhibition (Hollman & Morgan, 1997). However, the HG task used in this previous study was not of short duration. Therefore a build up of metabolites at the muscle, and subsequent activation of Type III and IV afferents, could have been responsible for or contributed to a portion of their results, and not necessarily stimulation of Type I and II muscle afferents. In addition, the involvement of cortical structures responsible for the observed sympatho-inhibition was not studied.

Based on the literature, there is evidence that regions of the CAN make shared contributions to autonomic control of HR and HRV. The vMPFC, ACC and insula all appear to be involved during tasks such as HG and STIM. However, despite these shared regions of control, HG and STIM appear to have opposing effects on HR and HRV.

Therefore, the primary **purpose** of this study was to determine whether stimulation of Type I and II afferents would modulate changes in HR and HRV associated with HG exercise. We tested the primary **hypothesis** that STIM would modulate HG-induced changes in HR and HRV. As a secondary **purpose**, with the use of functional MRI, we aimed to determine whether HG+STIM would reveal different cortical activation patterns within the CAN compared to either paradigm on its own. We tested the secondary **hypothesis** that areas within the CAN would produce different activation/deactivation patterns when STIM and HG are coupled compared to either paradigm on its own. Based on our hypotheses, our expected outcomes were:

a) HG alone would result in an increase in HR and decrease in HRV, with subsequent deactivation within the vMPFC and subgenual ACC, and activation within the anterior insula.
b) STIM alone would result in a decrease in HR and an increase in HRV, with subsequent activation within the vMPFC, posterior insula, and subgenual ACC.
c) HG+STIM would result in an attenuation of the HR and HRV responses to HG. Subsequently, activation of the anterior insula and deactivation of the vMPFC, would also be attenuated.

CHAPTER 2 – LITERATURE REVIEW

Physiological adjustments, at rest and in response to exercise, have been documented for years. The autonomic nervous system (ANS) is largely responsible for the regulation of visceral functions and the maintenance of internal homeostasis. In turn, cardiovascular adjustments to blood pressure (BP), heart rate (HR) and cardiac output are continuously and tightly controlled by the ANS.

2.1 Autonomic Characteristics

The autonomic nervous system is comprised of two major neural divisions: the parasympathetic nervous system (PNS) and the sympathetic nervous system (SNS). The cell bodies of both efferent systems originate from the central nervous system (CNS) and leave via cranial nerves or ventral roots to synapse with second-order ganglia, which give rise to axons that directly innervate smooth and cardiac muscle (Shields, 1993).

2.1.1. Sympathetic Nervous System

The cell bodies of the sympathetic efferent system lie in the intermediolateral (IML) cell column of the spinal cord between T1-L2 (Loewy, 1981). The short preganglionic neurons release acetylcholine (Ach) onto second order neurons, which allows for an efferent signal to continue down a long post-ganglionic neuron to its target tissue where it releases norepinephrine to bind to an alpha and/or beta-adrenergic receptor.

2.1.2. Parasympathetic Nervous System

A major source of parasympathetic outflow comes from cranial nerve X, the vagus nerve. The parasympathetic neurons of the vagus are located in the nucleus ambiguus and the dorsal motor nucleus. Like the SNS, the parasympathetic efferent system is comprised of two neurons. A long pre-ganglionic neuron, which releases Ach to bind to cholinergic nicotinic receptors on a second order neuron, and a short post-ganglionic neuron which releases Ach onto cholinergic muscarinic receptors located on the target tissue. Like many organs of the body, both branches of the ANS innervate the heart.

2.2. Autonomic Control of the Heart

The parasympathetic and sympathetic branches affect both cardiac rate and cardiac contractility through innervation at the sinoatrial and atrioventricular nodes, respectively. Ach release from the vagus nerve acts on M2 muscarinic receptors on the sinoatrial node, which causes an increase in cell membrane potassium conductance. This evokes hyperpolarization of the atrial cells, and thus decreased heart rate (HR) and contraction velocity (Pott & Pusch, 1979). The sympathetic influence on HR is mediated by the release of norepinephrine, and circulating epinephrine released by the adrenal medulla. Activation of beta-adrenergic receptors causes an increase in cyclic AMP, and in turn, increases calcium influx. The end result is an accelerated depolarization, ultimately increasing the cardiac rate and contractility. Although it is difficult to get direct measures of parasympathetic and sympathetic activity occurring at the heart, both divisions of the ANS can be indirectly measured in order to better understand their function.

2.4. Measuring parasympathetic activity

Parasympathetic activity cannot be measured directly through non-invasive methods. Therefore, researchers must rely on indirect measures to interpret parasympathetic outflow. Some techniques that have allowed researchers to indirectly measure and interpret vagal activity have included resting heart rate, heart rate recovery, baroreflex sensitivity, and heart rate variability.

2.4.1. Resting Heart Rate

Resting heart rate is a simple non-invasive indicator of autonomic balance. Despite a dynamic balance between both neural systems at rest, cardiovagal activity dominates HR control. Jose and Collison (1970) pharmacologically blocked both vagal and sympathetic receptors with atropine and propranolol, respectively. During the double blockade, the intrinsic HR was higher than the normal resting HR (Jose & Collison, 1970). Therefore, under normal resting conditions, the heart is under tonic inhibitory control by parasympathetic influence.

2.4.2. Heart Rate Recovery (HRR)

The ANS and cardiovascular system are closely linked. The increase in HR that accompanies exercise onset is largely caused by vagal withdrawal followed by increased sympathetic activity (Maciel, Gallo Jr., JA, & Martins, 1987). Heart rate recovery (HRR) is the ability of the cardiovascular system to return to resting levels at exercise cessation. When exercise stops, the period of recovery is characterized by a combination of sympathetic withdrawal and vagal reactivation in order to slow HR back to resting levels. Thresholds for a normal HRR are >12 beats at 1 minute of recovery for an upright position (Cole, Blackstone, Pashkow, Snader, & Lauer, 1999). An abnormal HRR is defined as a slowed decline of HR at exercise cession. The slowed HRR typically is attributable to defects in parasympathetic reactivation, sympathetic withdrawal, or both (Okutucu, Karakulak, Aytemir, & Oto, 2011). Therefore, it is suggested that abnormal HRR may act as a surrogate for underlying

autonomic dysfunction. In contrast, a normal HRR (<12bpm) at exercise cessation is representative of parasympathetic reactivation.

2.4.3. Baroreflex Sensitivity (BRS)

The evaluation of baroreflex sensitivity (BRS) is an established tool for autonomic control assessment. BRS represents the responsiveness of the cardiovascular system to adjust HR in response to blood pressure (BP) changes. In addition, the baroreflex system plays a dominant role in preventing wide fluctuations in the variability around arterial BP (Alper, Jacob, & Brody, 1987). Activation of the arterial baroreceptors in response to a rise in systemic BP leads to an increased discharge of parasympathetic neurons, and a decrease in sympathetic neuron discharge. This results in bradycardia and decreased cardiac contractility. Conversely, a decrease in systemic pressure leads to vagal inhibition and an increase of sympathetic neuron discharge, leading to tachycardia and increased cardiac contractility. There are significant differences in the time delay of the response mediated by vagal and sympathetic efferent activities. Vagal activation produces an estimated 400-600msec reaction (Petro, Hollander, & Bouman, 1970; Borst, Hollander, & Bouman, 1972), whereas sympathetic activation occurs much slower (3-6 sec) (Toda & Shimamoto, 1968). An even slower response has been observed in the baroreflex control of venous return (Shoukas & Sagawa, 1973). Therefore, the ability of the baroreflex to control HR on a beat-by-beat basis is primarily mediated through vagal activity.

2.4.4. Heart Rate Variability

Heart rate variability (HRV) represents the beat-to-beat oscillations in HR that seem to reflect a dynamic response of cardiovascular control systems to various physiological perturbations. High HRV demonstrates more frequent spontaneous fluctuations of HR, and a more complex interplay between the neural regulatory outflows. Experiments using pharmacological blockade of sympathetic and parasympathetic inputs to the sinoatrial node have demonstrated that nearly all HR fluctuations are mediated by efferent activity from these branches of the ANS (Akselrod, Gordon, Ubel, Shannon, Barger, & Cohen, 1981; Pagani, et al., 1986; Pomeranz, et al., 1985). The intervals between normal sinus beats can also vary as a result of respiration, BP regulation, thermoregulation, and many other unknown factors. In clinical applications, HRV is used as a marker of cardiovascular and autonomic health (Malik, et al., 1996). In contrast, low HRV is often a strong predictor of cardiovascular disease and all-cause mortality (Malik, et al., 1996). There are two approaches for measuring HRV, analysis in the time domain and the frequency domain.

2.4.4.1. Measuring HRV

Time Domain

The time domain approach analyzes the variations in instantaneous HR (HR at any given time) or intervals between successive normal beats. In order to calculate HRV in the time domain all abnormal beats must be removed, allowing only normal QRS complexes to remain to be analyzed (Billman, 2011). The normal-to-normal

intervals (NN) or instantaneous HR can be used to calculate simple time-domain variables such as the mean NN interval, the mean HR, and the difference between longest and shortest NN interval. Further statistical analysis can be applied to calculate the standard deviation of the NN (SDNN), which is one of the most widely used expressions of HRV in the time domain (Kleiger, Mille, Bigger, & Moss, 1987). SDNN reflects all the cyclic components responsible for variability in the period of recording (Malik, et al., 1996). SDNN is typically calculated over 24h recording periods, and therefore encompasses high frequency components and the lowest frequency components seen in a 24h period, which can easily be compared against other SDNN measures of the same recording period. However, as the recording period becomes shorter, the total variance of HRV also decreases (Malik, et al., 1996). Therefore, comparing SDNN measures obtained from recording periods of different durations would be inappropriate because of its dependence on the length of recording period. Therefore, SDNN would not be well suited for this thesis work due to the varying recording lengths.

Frequency Domain

Analysis in the frequency domain yields information regarding the amount of overall variability in HR, and provides information of how power (i.e. variance) distributes as a function of frequency. This is accomplished using a standard three-lead ECG to calculate the distance between consecutive R-R intervals (Figure 2. 1), which can then be submitted to a Fourier transform. A Fourier transform decomposes the time series of R-R intervals (Figure 2. 2) into a sum of sinusoidal

frequencies and amplitudes, and a power spectrum is then computed to reflect the amplitude of fluctuations at different frequencies (van Ravenswaaij-Arts, Kollee, Hopman, Stoelinga, & van Geijn, 1993) (Figure 2. 3). There are three main spectral components that can be calculated from short-term recordings of 2 to 5 minutes: the high frequency (HF) component (0.15-0.4Hz), which is suggested to reflect primarily vagal activity, the low frequency (LF) (0.04-0.15Hz), suggested to reflect both sympathetic and vagal activity (Malik, et al., 1996; Pomeranz, et al., 1985), and very low frequency (VLF) (0.0033-0.04Hz), which is often the most disputed, but is suggested to be representative of the renin-angiotensin system (Akselrod, Gordon, Ubel, Shannon, Barger, & Cohen, 1981), or thermoregulatory effects (van Ravenswaaij-Arts, Kollee, Hopman, Stoelinga, & van Geijn, 1993).

Typically, spectral analysis requires steady-state conditions, and recording periods of 5 minutes or more (Toledo, Gurevitz, Hod, Eldar, & Akselrod, 2003). However, due to the nature of our protocol where rest and task conditions change repeatedly and each condition lasts less than one minute, wavelet analysis of HRV was used to measure time-varying and non-stationary data (Samar, Bopardikar, Rao, & Swartz, 1999; Torrence & Compo, 1998).

A wavelet based spectral approach adapts similar characteristics of the Fourier transform. However, it also uses a mother wavelet to extract specified waves oscillating at various frequencies. In addition, rather than a frequency-power distribution, a wavelet based spectral approach performs a time-frequency decomposition of the HR signal and yields a time-dependent component of the LF and HF peaks (Toledo, et al., 2003). This method provides information on autonomic

control, as reflected by HRV, over short periods of potentially non-stationary data, allowing determination of how frequency distributes as a function of time. Therefore, it is possible to see at what time during data collection were there changes in HRV, and at what frequencies were such changes occurring.

Respiratory Sinus Arrhythmia (RSA)

During normal spontaneous breathing, HR is in synchrony with respiration. Respiratory sinus arrhythmia demonstrates shortened R-R intervals during inspiration and lengthened intervals during expiration (Yasuma & Hayano, 2004). The mechanisms responsible for the respiratory modulations are not completely understood. However, Chess and colleagues (1975) demonstrated that such changes are mediated principally through the vagus nerve (Chess, Tam, & Calaresu, 1975). In support of their findings, RSA can also be abolished by atropine or vagotomy. More over, respiration and HF-HRV are intimately linked, which is evident by the removal of the HF component of HRV during inspiratory apneas (Van De Borne, et al., 2001).

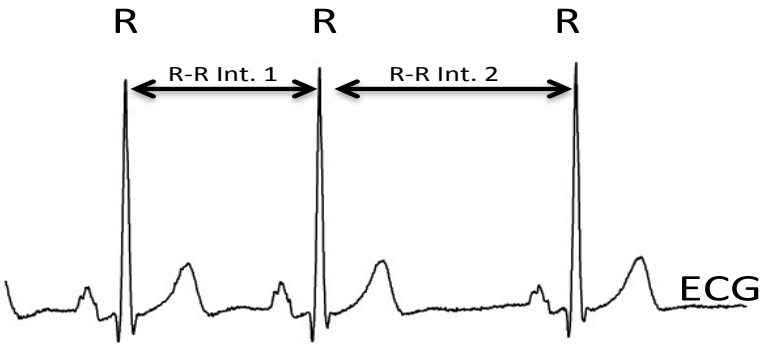

Figure 2. 1: Schematic representation of R-R intervals taken from an ECG recording.

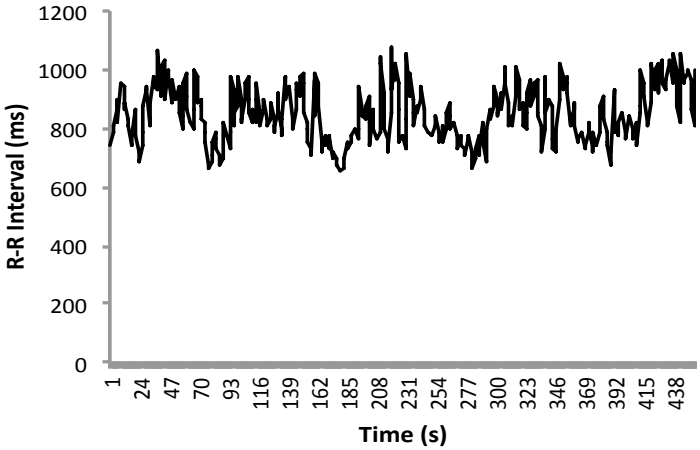

Figure 2. 2: A series of R-R intervals plotted against time from a recording session

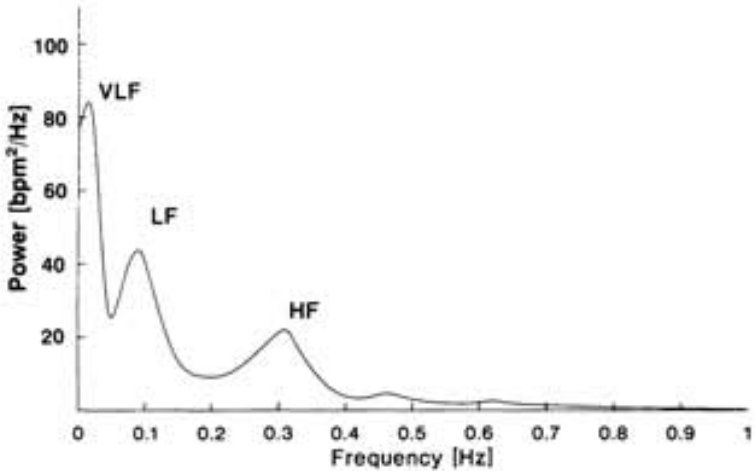

Figure 2. 3: Decomposition of R-R intervals into a power spectrum at high, low, and very low frequencies.

(Source: van Ravenswaaij-Arts CMA, Kollee LAA, Hopman JCW, Stoelinga GBA, and van Geijn HP. Heart rate variability. *Annals of Internal Medicine* 118: 437-447, 1993. Used with permission by *Annals of Internal Medicine*)

2.5. Isometric Handgrip Exercise

2.5.1. Cardiovascular Effects of Isometric Exercise

Cardiovascular responses to voluntary muscular contraction include increases in HR, BP, and cardiac output (Lind, Taylor, Humphreys, Kennelly, & Donald, 1964). Percentage of maximal voluntary contraction (MVC) is an important element to determine cardiovascular responses. During contractions less than 15% MVC, a new cardiovascular steady state may develop. In contrast, sustained handgrip contractions greater than 15% MVC, will elicit an increase in HR, BP, and cardiac output that all rise in an approximately linear fashion until muscular fatigue (Lind, Taylor, Humphreys, Kennelly, & Donald, 1964; Lind & McNicol, 1967).

2.5.2. Cardiovascular Control Mechanisms during Isometric Exercise

For decades, research has looked at the mechanisms that serve to initiate the increases in HR, BP and cardiac output in response to isometric exercise. The rapid onset of the cardiac changes during isometric exercise strongly suggests a neurogenic mechanism (Petro, Hollander, & Bouman, 1970; Borst, Hollander, & Bouman, 1972). Muscular contraction is almost instantaneously followed by HR acceleration (Petro, Hollander, & Bouman, 1970; Borst, Hollander, & Bouman, 1972). The initial increase in HR is largely attributed to vagal withdrawal (Maciel, Gallo Jr., JA, & Martins, 1987), and the presence of acetylcholinesterase. Acetylcholinesterase is thought to be the fastest enzyme in the body, and following vagal withdrawal, rapidly begins to break down any residual Ach, which accounts for the speed of the HR response. Unlike vagal withdrawal, there is a latency of 3-6

seconds between sympathetic nerve stimulation and the measured HR acceleration (Toda & Shimamoto, 1968). Therefore sympathetic activation would be too slow to account for the speed of the early HR response. In addition, the bulk of this initial (<10s) HR response can be blocked using the parasympathetic blocker, atropine, but not the sympathetic blocker, propranolol (Maciel, Gallo Jr., JA, & Martins, 1987). Finally, in a two-minute 30% sustained contraction, there were no changes in sympathetic activity, measured by muscle sympathetic nerve activity, during the first minute of exercise, despite an almost instant HR response (Mark, Victor, Nerhed, & Gunnar Wallin, 1985). Contractions at higher intensities (>50%) still evoke an initial HR response via parasympathetic withdrawal, but also a sympathetic response that arises much sooner (Maciel, Gallo Jr., JA, & Martins, 1987).

2.6. Ascending Neural Signals

2.6.1. Muscle Sensory Afferent Characteristics

There are four types of muscle sensory nerves found within each muscle nerve innervating skeletal muscle. Each fiber relays information back to the brain regarding activity at the muscle. Type I fibers are large diameter fibers with thick myelination. These fibers have fast conduction velocities (72-120m/s), and arise from muscle spindles (Ia) and the Golgi tendon organs (Ib). Type II fibers have less myelination, are slower (31-71 m/s) compared to Type I, and arise from secondary muscle spindles. The thinly myelinated Type III, and unmyelinated Type IV have very slow conduction velocities (2.5-30 m/s and < 2.5 m/s, respectively), and

terminate as free nerve endings in the skin and skeletal muscle (Kaufman and Hayes, 2002).

2.6.2. Muscle Sensory Afferents in Cardiovascular Control

For over 70 years, experimental evidence has supported the hypothesis that a reflex pressor response to exercise can partly be maintained if arterial and venous blood is trapped in the contracting muscle (Alam & Smirk, 1937; Kaufman & Hayes, 2002). Subsequent research has highlighted Type III and IV fibers as the afferents responsible for the cardiovascular arousal and respiratory functions that come from muscle during exercise (McCloskey & Mitchell, 1972). Type III fibers are rapidly (2-5s) excited by mechanical distortion of the muscle (Adreani, Hill, & Kaufman, 1997), with a few responsive to chemical stimuli. Type IV afferents are predominantly excited by chemical changes, such as metabolite accumulation, with some sensitive to mechanical distortion (Kaufman, Longhurst, Rybicki, Wallach, & Mitchell, 1983; Kaufman, Rybicki, Waldrop, & Ordway, 1984). As such, Type IV afferents typically have a delayed response (5-20s) compared to Type III afferents (Kaufman, Rybicki, Waldrop, & Ordway, 1984).

Substantial evidence indicates that Type III and IV, but not I and II are responsible for the cardiovascular arousal evoked by muscular contraction (Kaufman, Rybicki, Waldrop, & Ordway, 1984; Kaufman, Longhurst, Rybicki, Wallach, & Mitchell, 1983; McCloskey & Mitchell, 1972). However, unlike Type III and IV afferents, the role of Type I and II fibers in cardiovascular control has not fully been elucidated. Some research using electrical nerve stimulation has implicated Type I and II afferents in

an inhibitory cardiovascular autonomic role (Hollman & Morgan, 1997; Owens, Atkinson, & Lees, 1979). The technique of nerve stimulation has proven to be a useful tool for investigating the role of Type I and II fibers in autonomic regulation. Electrical nerve stimulation relies on the different cable properties of muscle afferents for selective recruitment.

2.7. Somatosensory Electrical Nerve Stimulation (SSNS)

2.7.1. Selective Nerve Recruitment

Electrical nerve stimulation that is carefully graded can be used to selectively stimulate afferent fibers based on diameter. Peripheral nerve stimulation has characterized large diameter, fast conducting fibers as having the lowest stimulation threshold (Swett & Bourassa, 1981). This occurs because larger diameter fibers exhibit less resistance to current flow. Thus, large diameter muscle afferents (Type I and II) can be recruited at low stimulation intensities, whereas the thinly myelinated and unmyelinated small fibers are not recruited until higher stimulation intensities. The method of nerve stimulation is not new. Prior to research in autonomic regulation, electrical nerve stimulation was used as a pain management modality.

2.7.2. Gate Control Theory of Pain

Transcutaneous electrical nerve stimulation has been used in pain management for over 20 years. The 'gate control theory of pain' proposed by Melzack and Wall in 1965 helps to explain the effectiveness of this technique. Melzack and Wall (1965)

suggested the rate of action potential afferent information from nociceptor to the CNS could be regulated by other afferent signals coming into the spinal cord at the same level (Melzack and Wall, 1965). In addition, this regulatory mechanism is controlled by activity in both large and small fibers. Large diameter fibers, such as Type I and II, inhibit the afferent signals, whereas small fibers, such as Type III and IV, facilitate afferent signals (Moayedi & Davis, 2013). For the purpose of this thesis, we applied somatosensory stimulation (STIM) to investigate whether ascending afferent signals from Type I/II fibers would modulate descending efferent motor signals activated by HG exercise.

2.7.3. Effects of STIM on Autonomic Control

Despite its roots in pain therapeutics both high and low frequency STIM are used to study the effects of somatosensory stimulation on autonomic responses. For example, Owens et al. (1997) applied STIM (75Hz) to the median nerve of healthy subjects, and reported increased skin temperature. They concluded their results represented indirect evidence of cutaneous vasodilation, which in turn was attributed to decreased sympathetic tone (Owens, Atkinson, & Lees, 1979). Hollman and Morgan used muscle sympathetic nerve activity to measure sympathetic activity during a pressor response to 25% sustained isometric HG. When STIM (60Hz) was applied to the ipsilateral forearm, the sympathetic response to fatiguing HG exercise was blunted, detectable through decreased sympathetic burst frequency. In addition, systolic BP was also attenuated. The suggested mechanism was that central transmission of neural impulses from Type III and IV afferents were

regulated by other afferent inputs converging at the same spinal level (Hollman & Morgan, 1997). In another sustained HG study, participants maintained 30% of their MVC for 2 minutes with and without STIM. Diastolic BP was attenuated when STIM was applied compared to the control test (Sanderson, et al., 1995).

In addition, STIM represents a possible intervention to help reduce sympathetic hyperactivity, and restore sympatho-vagal balance. For example, periodic STIM (80Hz) applied to both feet of chronic heart failure (CHF) patients resulted in a 28% increase in BRS that was also maintained after the intervention session was completed. The authors concluded that somatosensory inputs alone were efficient and sufficient to increase the BRS in CHF patients (Gademan, et al., 2011). In hypertensive persons, four weeks of low frequency STIM (1.7Hz) applied over the dorsal web of the first and second metacarpals decreased both mean systolic and diastolic BP. In addition, this effect was still present at least one week later during the post-stimulation period. The authors attributed these effects to central inhibition of sympathetic activity (Jacobsson, Himmelmann, Bergbrant, Svensson, & Mannheimer, 2000). Similar to Jacobsson and colleagues (2000), Kaada (1991) used low frequency STIM (2Hz), and applied the therapy to patients with mild and moderate hypertension. As a result, there were significant reductions in systolic, mean arterial and diastolic pressures. After two weeks of daily stimulation, BPs remained low in the post-stimulation period (Kaada, Flatheim, & Woie, 1991). Most research using STIM has attributed the results to sympatho-inhibition, and to complement this idea, recent work using somatosensory stimulation and functional

MRI has demonstrated representations of somatosensory inputs within the cortical autonomic network (CAN) (Goswami, Frances, & Shoemaker, 2011).

2.8. The Cortical Autonomic Network

The cortical autonomic network (CAN) has been exposed by clinical and neuroimaging studies as a network of forebrain regions associated with autonomic control. As noted above, the ventral medial prefrontal cortex (vMPFC), the anterior cingulate cortex (ACC), and the insular cortex are some key cortical structures that make up the CAN (Verberne & Owens, 1998; Kimmerly, O'Leary, Menon, Gati, & Shoemaker, 2005; Wong, Masse, Kimmerly, Menon, & Shoemaker, 2007b).

2.8.1. Ventral medial prefrontal cortex

It is well established that the vMPFC (Figure 2. 4) plays an important role in autonomic regulation. In a rat model, electrical stimulation applied to the vMPFC has identified depressor sites (Fisk & Wyss, 1997; Owens & Verberne, 2001), which upon stimulation cause sympatho-inhibition detected by hypotension and bradycardia (Fisk & Wyss, 1997). In addition, neuronal recordings of the rostral ventrolateral medulla, an area that contains premotor sympatho-excitatory neurons (Guyenet, 1990), demonstrated inhibited discharge during vMPFC stimulation (Verberne, 1996). In monkeys, neuronal recordings within the vMPFC demonstrated a marked increase in neuronal firing when monkeys were in a vegetative state (i.e. asleep) compared to an awakened state (Rolls, Inoue, & Browning, 2003). These findings in animals have been extended to research with humans. Functional MRI data from 49 subjects were collected while they rested quietly, but awake with their

eyes closed. During the rested state, there was enhanced activation of the vMPFC compared to a task-induced state (Raichle, MacLeod, Snyder, Powers, Gusnard, & Shulman, 2001). A similar study used MR imaging to analyze brain activity on 26 subjects during a rested state, and ECG data to calculate HRV. The results indicated a positive covariation of the BOLD signal within the vMPFC and RR interval (Ziegler, Dahnke, Yeragani, & Bar, 2009). Furthermore, neuroimaging during HG exercise also highlighted the vMPFC as a structure highly correlated with parasympathetic activity. Specifically, during a short-duration HG task, brain patterns reveal progressive deactivation of the vMPFC that correlated with a concurrent increase in HR in response to exercise. In contrast, during the recovery phase, the vMPFC became increasingly activated as HR returned to baseline levels (Wong, Masse, Kimmerly, Menon, & Shoemaker, 2007b). The HR response to graded short duration isometric HG was correlated with deactivation in the vMPFC. A stronger level of deactivation was observed as participants completed higher intensity HGs that elicited higher HR responses (Wong et al. 2007).

In addition, the vMPFC was also positively correlated with an increase in HF-HRV during sub-motor somatosensory stimulation (Goswami, Frances, & Shoemaker, 2010). These findings in both animal and human models suggest the vMPFC may be associated with parasympathetic activity (Critchley, 2004).

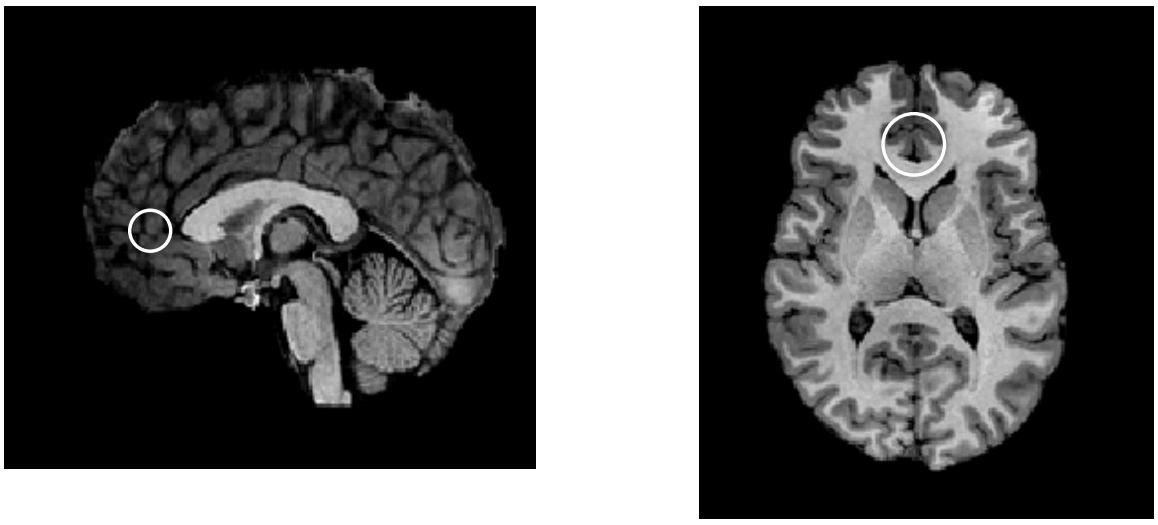

Figure 2. 4: Sagittal (left) and transverse (right) view of the ventral medial prefrontal cortex.

2.8.2. Anterior Cingulate Cortex

The anterior cingulate cortex (ACC) lies dorsal, rostral and ventral to the corpus callosum (Devinsky, Morrell, & Vogt, 1995). In addition to behaviour and cognitive function such as choice selection and response inhibition (Devinsky, Morrell, & Vogt, 1995; Matthews, Paulus, Simmons, Nelesen, & Dimsdale, 2004), the ACC plays a significant role in autonomic function. Kaada (1951) reported both pressor and depressor responses as a result of electrical stimulation to the ACC (Kaada B. , 1951). The most likely explanation for this finding is that the ACC has several functional subdivisions.

One such subdivision, the subgenual ACC (Figure 2. 5A), contains extensive connections with autonomic centers including the nucleus tractus solitarius (Terreberry & Neafsey, 1983) and the dorsal motor nucleus of the vagus (Hurley, Herbert, Moga, & Saper, 1991), supporting the role of the subgenual ACC in PNS activity. In addition, activation of this area was correlated with HF-HRV during a cognitive challenge (i.e. Stroop task), and in response to somatosensory stimulation (Goswami, Frances, & Shoemaker, 2011). This literature demonstrates a parasympathetic modulatory role of the subgenual ACC (Matthews, Paulus, Simmons, Nelesen, & Dimsdale, 2004).

In contrast, the dorsal ACC (dACC) (Figure 2. 5B) is an area related to sympathetic modulation of cardiac function during both effortful cognitive and motor tasks (Critchley, et al., 2003). During a HG task, there were large clusters of activation within the dACC. In addition, HRV measurements indicated the dACC was associated with increasing LF power (Critchley, et al., 2003), which the authors attributed to an

increase in sympathetic activity. Macefield and colleagues used a maximal inspiratory apnea to induce a large increase in spontaneous muscle sympathetic nerve activity. When the inspiratory muscles were virtually silent during the static phase of the maneuver, there was significant BOLD signal activity in the dACC that correlated with the sympathetic stressor (Macefield, Gandevia, & Henderson, 2006).

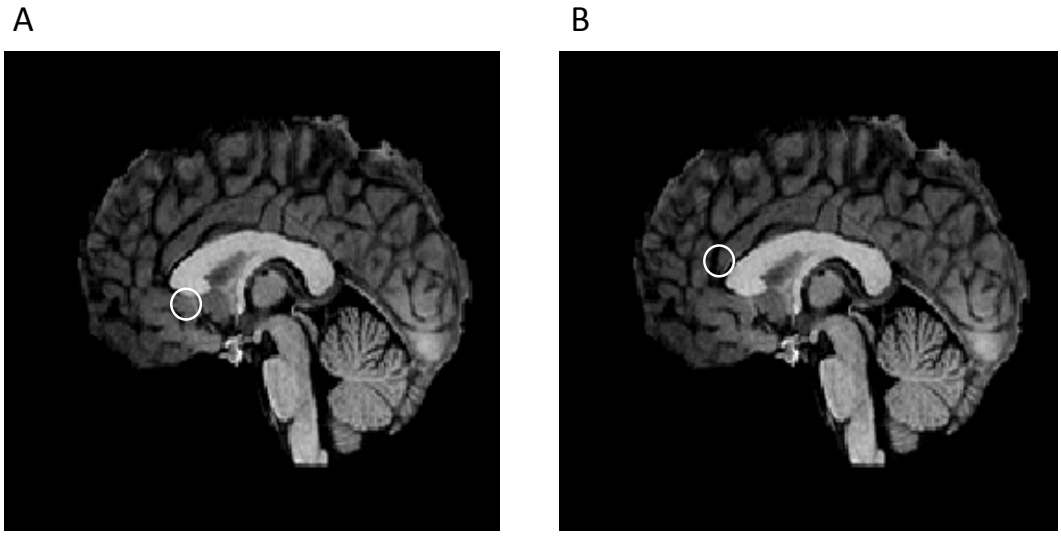

Figure 2. 5: Sagittal views of the subgenual (left) and dorsal (right) anterior cingulate cortices.

2.8.3. Insular Cortex

The insular cortex lies buried in the lateral sulcus, and can only be visualized by retracting the frontal, temporal and parietal opercula (Figure 2. 6). The anterior and posterior regions of the insula are separated by the central insular sulcus where the main branch of the middle cerebral artery lies (Flynn, Benson, & Ardila, 1999). Research looking at the role of the insula in cardiovascular function has shown that any autonomic influences are largely dependent on the insular region under investigation. For example, electrical stimulation of the insula of rats resulted in tachycardia represented in the rostral posterior insula, and bradycardia in the caudal posterior insula (Oppenheimer & Cechetto, 1990). In humans, electrical stimulation of the right insula evoked a tachycardic and pressor response, whereas left insular stimulation resulted in bradycardia (Oppenheimer, Gelb, Girvin, & Hachinski, 1991). The left insula has also been correlated with HF-HRV during emotion (Lane, McRae, Reiman, Chen, Ahern, & Thayer, 2009) and working memory tasks (Gianaros, Van Der Veen, & Jennings, 2004), suggesting an association of the left insula with parasympathetic activity.

In addition to lateralization, the insula cortex can also be divided into anterior, mid, and posterior regions (Macey, et al., 2012; Kurth, Eickhoff, Schleicher, Hoemke, Zilles, & Amunts, 2009). Neuroimaging studies reveal bilateral activation of the anterior and mid insular regions in response to sympatho-excitatory tasks (King, Menon, Hachinski, & Cechetto, 1999; Macefield, Gandevia, & Henderson, 2006). In addition, bilateral activation of the anterior and mid insula, as well as vMPFC

deactivation, was thought to modulate the HR increase in response to isometric HG exercise (Wong, Masse, Kimmerly, Menon, & Shoemaker, 2007b).

Neuron recordings have demonstrated both sympatho-excitatory and sympatho-inhibitory neurons in the right posterior insula of primates during pharmacologically induced BP challenges (Zhang, Dougherty, & Oppenheimer, 1998). In humans, right posterior insula activation was observed during lower body negative pressure (LBNP) when muscle sympathetic nerve activity and HR increased (Kimmerly, O'Leary, Menon, Gati, & Shoemaker, 2005). In addition, Critchley et al., (2000) found right posterior insula activation during a sustained isometric HG task (Critchley, Corfield, Chandler, Mathias, & Dolan, 2000). However, during both LBNP and HG, researchers only measured HR changes, which can be attributed to PNS withdrawal and SNS activation. Therefore, instead of HR, Napadow et al. (2008) measured HRV in response to HG exercise. During the HG task the left posterior insula was positively correlated with the HF component of HRV, an index of parasympathetic activity (Napadow, Dhond, Conti, Makris, Brown, & Barbieri, 2008). Lastly, bradycardia and increased R-R intervals were reported during electrical stimulation of the left posterior insula in humans (Oppenheimer, Gelb, Girvin, & Hachinski, 1991) Therefore, contrary to the anterior and mid regions of the insula, the left posterior insula may have a greater role in PNS activity than SNS activity.

In addition to cardiovascular 'motor' paradigms, the insula is also involved in somatosensory processing. It has been demonstrated that somatosensory inputs project directly and indirectly to the posterior insula in rats (Zhang & Oppenheimer,

2000) and monkeys (Zhang, Dougherty, & Oppenheimer, 1999). Also in humans, the posterior insula demonstrated bilateral activation during sub-motor somatosensory stimulation (Goswami, Frances, & Shoemaker, 2011). This coincides with other literature that has also highlighted the posterior insula cortex as a region that plays an important role as a somatosensory association area (Augustine, 1996; Burton, Videen, & Raichle, 1993). The concept that somatosensory information is processed within the posterior insula, and the CAN in general, is particularly important for this study, as we look at the effects STIM may have on autonomic regulation.

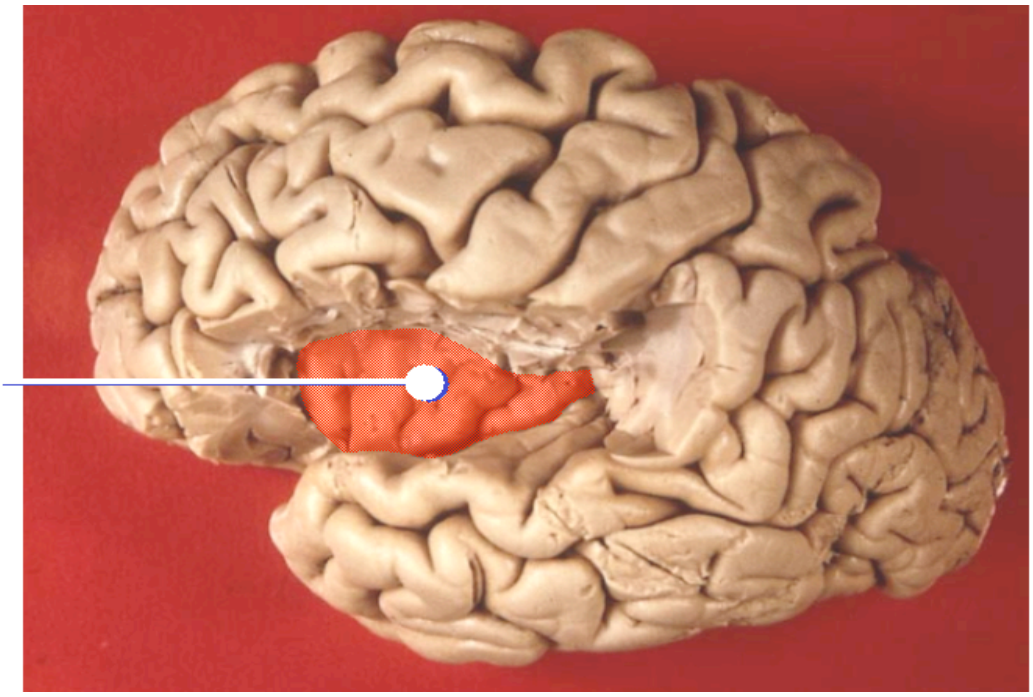

Figure 2. 6: View of the insula cortex buried beneath the frontal, temporal, and parietal lobes.

(Source: http://www.healcentral.org/healapp/showMetadata?metadataId=40566. By John A. Beal, PhD. Department of Cellular Biology & Anatomy, Louisiana State University Health Sciences Center Shreveport)

2.9. Collection Modalities

The advent of magnetic resonance imaging (MRI) technology has enhanced research and medicine alike, offering a non-invasive technique that has enabled researchers to gain essential clinical information, and insight into the basic mechanisms of brain function.

2.9.1. Functional Magnetic Resonance Imaging

MRI can measure any nuclei with an odd number of neutrons. Therefore, because hydrogen (^1H) is highly abundant in the body (H_20), it yields a large signal that can easily be measured. In the body, ^1H protons are randomly oriented and possess nuclear spin. However, when an external magnetic field (B_0) is applied, the ^1H atoms will randomly align parallel or anti-parallel to the direction of the B_0 (parallel>anti-parallel) (Brown, Perthen, Liu, & Buxton, 2007). The key to MRI is that the ^1H nuclei vary in strength depending on their surroundings, i.e. grey matter, white matter, cerebral spinal fluid, etc. When an additional magnetic field (B_1) is applied perpendicular to B_0, it causes the magnetization of the protons to be tipped away from B_0. A radio frequency (B_1) applies a pulse that rotates the protons at a given angle, known as the flip angle. When this occurs, the original magnetization is split into longitudinal and transverse components (Brown, Perthen, Liu, & Buxton, 2007). When the B_1 pulse is shut off, the protons begin to relax, and the longitudinal component of magnetization returns exponentially to its equilibrium state. The time it takes for the protons to realign with the main magnetic field (B_0) is referred to as the time constant, T_1. A T_1-weighted anatomical image is the most popular

anatomical image. The transverse component decays exponentially with a transverse relaxation referred to as the time constant, T_2 (Logothetis, 2002; Brown, Perthen, Liu, & Buxton, 2007). T_2 refers to relaxation in a perfectly homogenous magnetic field – a field that doesn't exist because magnetic inhomogeneities are inherent in functional imaging. Therefore a time constant of T_2* is measured which reflects the effective transverse relaxation time (Logothetis, 2002).

Functional MRI (fMRI) provides a tool for mapping brain patterns of activation and deactivation through detection of changes in blood oxygenation and blood flow that occur in response to neural changes. When areas of the brain become activated, the demand for more oxygen leads to an increase in blood flow. The blood-oxygen-level-dependent (BOLD) response is the basis for most fMRI studies, first described by Ogawa and colleagues (1990). In a rodent model, they discovered a contrast mechanism in the blood between oxyhemoglobin (Hb) and deoxyhemoglobin (dHb). The difference in magnetic properties between Hb, which is diamagnetic, and dHb, which is paramagnetic, led to distinct differences in MR signaling. In addition, the paramagnetic properties of dHb are confined within the intracellular space of red blood cells, that are in turn restricted to blood vessels. Consequently, allowing for differences between dHb-containing compartments and the surrounding space to be detected (Logothetis, 2002).

Increased neuronal activity causes a hemodynamic response pattern that can take form in three distinct phases. 1) After the onset of the stimulus (2-3s), there is a small initial dip, also known as the fast response, due to the immediate metabolic consumption of oxygen without any changes in blood flow (Norris, 2006). 2) This is

followed by the main BOLD response peaking around 5 seconds, in which blood flow increases to a level beyond the metabolic rate of oxygen consumption. This causes the blood oxygenation to increase, dHb to decrease, and the MR signal to increase following neuronal activation (Norris, 2006). 3) The last phase is characterized by a post-stimulus undershoot that lasts about one-minute, in which there is a delayed return of the blood volume to baseline while oxygen consumptions remains slightly elevated (Norris, 2006) (Figure 2. 7).

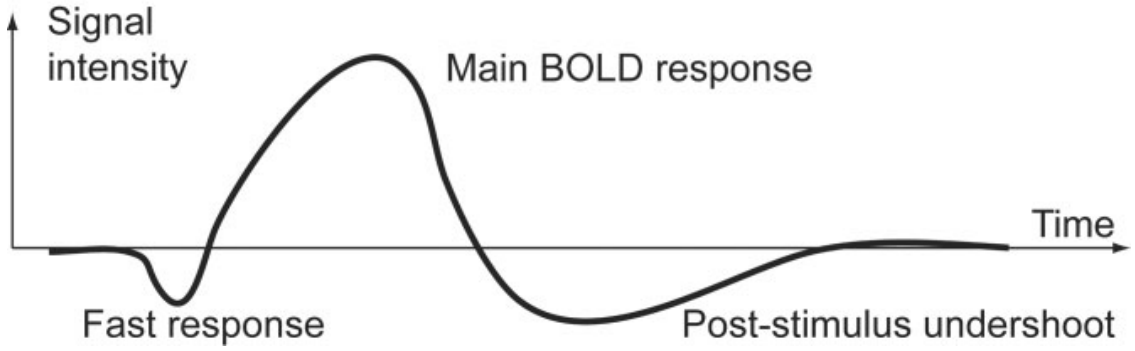

Figure 2. 7: Time course of the BOLD response to a stimulus.

(Source: Norris, D.G. Principals of Magnetic Resonance Assessment of Brain Function. *Journal of Magnetic Resonance Imaging* 23: 794-807, 2006. Used with permission by *Journal of Magnetic Resonance Imaging*)

Overall, the role of Type I and II muscle afferents in autonomic control has not been fully elucidated. However, selective stimulation by means of sub-motor electrical nerve stimulation offers a modality that could help shed some light on their autonomic role. In contrast, the physiological responses to isometric handgrip exercise have been more thoroughly investigated, with its effects on heart rate and rate variability seemingly opposite to those elicited by sub-motor somatosensory stimulation. Despite the seemingly opposing effects of sub-motor somatosensory stimulation and isometric handgrip exercise on heart rate and heart rate variability, there is overlap in their regions of autonomic regulation within the CAN, specifically within the vMPFC, ACC and insular cortices.

Therefore, the **purposes** of this study were to a) determine whether stimulation of Type I and II afferents would modulate changes in HR and HRV associated with HG exercise when both modalities are performed together, and b) with the use of functional MRI, determine whether HG+STIM produces different cortical activation patterns within the CAN compared to either paradigm on its own. We tested the primary **hypothesis** that STIM would modulate HG-induced changes in HR and HRV. We tested a secondary **hypothesis** that areas within the CAN would produce different activation/deactivation patterns when STIM and HG exercise are coupled compared to either paradigm on its own.

CHAPTER 3 – METHODS

3.1 Participants

Fifteen volunteers participated in this study. Two participants were excluded for non-compliance (1. Inability to maintain consistent handgrip intensity, 2. Unable to return for second visit), and a third participant was excluded due to high markers of cardiovascular risk (markers of inflammation) determined by blood sample analysis. Overall, twelve young, healthy participants completed this study (7 females, 5 males) (Table 3. 1). All participants were non-smokers, with no history of cardiovascular, musculoskeletal, metabolic or neurological diseases. All participants provided informed written consent to the experimental procedures that were approved by the Health Science Research Ethics Board at The University of Western Ontario.

Table 3. 1: Participant characteristics.

Characteristics	Value (mean ± SD)
Age (years)	24±2
Height (cm)	169±8
Weight (kg)	65±14
BMI (kg/m^2)	23±4
RHR (bpm)	58±8
Resting MAP (mmHg)	80±6

cm, centimeters; kg, kilograms; BMI, body mass index; kg/m^2, kilograms per meter squared; RHR, resting heart rate; bpm, beats per minute; MAP, mean arterial pressure; mmHg, millimeters of mercury.

3.2 Experimental protocol

The study consisted of two separate visits: One visit for physiological recordings at the Laboratory for Brain and Heart Health, and one magnetic resonance imaging (MRI) visit at Robarts Research Institute. During both visits, participants underwent sub-motor somatosensory stimulation (STIM) on their right arm, performed handgrip (HG) exercises with their left hand, and HG exercises concurrent with STIM (HG+STIM). The order of HG and STIM were randomized, and HG+STIM was always performed last.

3.3. Laboratory Session

Participants arrived at the laboratory after having been instructed to fast for at least 3 hours, and refrain from physical activity, caffeine and alcohol for at least 12 hours prior to testing. All participants were measured for height and weight prior to beginning the study. At least 1.5 hours prior to the start of testing, a Eutectic Mixture of Local Anesthetic (EMLA®) (AstraZeneca Canada Inc., Mississauga, ON) patch, a cutaneous sensory afferent blockade, was applied over the right forearm flexor muscle belly, detected by muscle palpation during forced wrist flexion. After the EMLA® patches were applied, participants lay supine for 30 minutes prior to a venous blood draw taken from the left antecubital vein for detection of resting catecholamine levels, fasting blood glucose, lipids, and other markers of cardiovascular health such as endothelium function and inflammation. Following blood draw, all participants were provided with a snack and juice/water while they provided information relating to their health history. In addition handedness was

determined according to the Edinburgh Handedness Inventory (Oldfield, 1971). Overall, ten of the twelve participants were right-handed. However, handedness was not a concern as previous research has demonstrated that handedness does not affect physiological responses to isometric handgrip exercise (Wong, et al., 2007b). At the start of the study, while supine, the EMLA® patches were removed, and cutaneous afferent blockade was verified by lightly touching the skin, while participants provided verbal feedback on the level of sensation. Two self-adhesive stimulation electrodes were then positioned over the muscle belly. Sub-motor threshold was determined by increasing the stimulation intensity until a contraction was observed (motor threshold), followed by lowering the intensity to a level just below the motor threshold. Sub-motor electrical nerve stimulation was used in order to selectively recruit large diameter Type I and II muscle afferents. Sub-motor stimulation settings were consistent across all participants and experimental trials, with a pulse frequency of 100Hz and pulse duration of 50μs.

3.3.1. Protocol

3.3.1.1 Protocol 1: Sub-motor Somatosensory Stimulation (STIM)

Participants were instructed to lie as still as possible for the duration of the first protocol. Participants were informed they would feel intermittent STIM on their right forearm throughout the protocol. After one minute of rest, a total of seven 30 second STIMs with a 15 second rest in between, were performed.

3.3.1.2 Protocol 2: Handgrip (HG) Exercise

Prior to performing the HG protocol, participants were instructed to perform two maximal voluntary contractions (MVC). The higher of the two MVCs was calibrated as 100%. Participants performed three blocks of HGs at 30, 40, and 50% of their MVC. All handgrip trials were performed with participant's left hand. Within each block, participants performed four HG trials, each lasting 20 seconds followed by one minute of recovery. In order for participants to maintain the desired HG intensity, participants were provided with continuous visual feedback during each HG exercise. After the completion of each block, participants were presented with a scale from 6 to 20 (Borg 1982) in order to determine their level of perceived exertion. In addition, participants were instructed to maintain a spontaneous breathing rhythm throughout each HG exercise.

3.3.1.3 Protocol 3: Handgrip Exercise and Sub-motor Stimulation (HG+STIM)

Prior to repeating the HG exercise, with the left hand, with concurrent STIM on the right arm, a third MVC was performed to ensure participants were not fatigued from the first HG protocol. Participants were given the same instructions as mentioned above. However, this time they were informed there would also be STIM applied to their right forearm during each 20-second HG exercise. Following each HG block, participants were again presented with the BORG scale to determine their level of perceived exertion during the HG exercise.

3.3.2 Physiological Recordings

Three adhesive electrodes were placed on the chest of each participant to record HR using a standard 3-lead ECG (Pilot 9200, Colin Medical Instruments, San Antonio, TX, USA). A sphygmomanometer was used to collect three manual blood pressures, which were averaged and used to calculate resting mean arterial pressure. A respiratory belt (ADInstruments, MLT1132 Piezo Respiratory Belt Transducer, Colorado Springs, CO, USA) was placed across each participant's abdomen to ensure participants were breathing spontaneously throughout the HG exercises, and to measure breathing frequency. We specifically isolated breathing frequency, within the HF domain, in order to best reflex vagal activity. All measurements were recorded and stored for later analysis (PowerLab, ADInstruments, Colorado Springs, CO).

3.3.3. Physiological Data Analysis

For all participants, HR was averaged for the last 30-seconds of each rest period, and the last 10-seconds of each HG trial during both HG and HG+STIM conditions. During the STIM procedure, HR was averaged for the last 10-seconds of each STIM trial, and last 10-seconds of each rest period. HRV was determined as an indirect measure of vagal activity. HRV was calculated by measuring the distance between R-R intervals, followed by a wavelet-based spectral analysis approach to produce power data ranging between frequencies of 0.1-0.4Hz (Toledo, et al. 2003). High-frequency HRV was determined as a frequency between 0.15-0.4Hz, corresponding to respiratory frequency modulations.

3.3.4 Statistical Analysis

The effect of STIM on average HR and HRV, as well as the average HR and HRV between HG and HG+STIM during the MRI session, were assessed using a two-tailed t-test. The effects of condition (HG and HG+STIM) and handgrip intensity (30, 40, and 50%) on heart rate and heart rate variability during the laboratory session were assessed using a 2x3 repeated measures ANOVA. The HRV data were normalized to the natural logarithm (ln) prior to statistical analysis. The significance level was set at $p<0.05$.

3.4. MRI Session

All twelve participants returned to the laboratory on a separate date for the MRI study. Again, they arrived 1.5 hours prior to testing in order to position the EMLA® patches over the right forearm flexor muscle belly. Participants were once again instructed to refrain from physical activity, caffeine and alcohol for at least 12 hours prior to testing. When participants arrived at the MRI suite for testing, the EMLA® patches were removed, and cutaneous blockade was confirmed. Data from eleven participants are presented in the neuroimaging results due to the loss of one participant's scans.

Each participant repeated the laboratory session protocols of STIM, HG and HG+STIM with some exceptions. First, in order to improve the signal-to-noise ratio (i.e. cortical activation signal relative to background noise), a total of seven instead of four HGs were performed with one minute of rest between each trial. Second, HG exercise was performed at 40% MVC only. This intensity was chosen based on the

laboratory results, which showed that 40%HG produced a significant HR response. In addition, at this intensity, STIM had the largest effect on HRV.

3.4.1. Physiological Data Collection

HR was acquired using an MRI-compatible pulse oximeter attached to the second finger on the right hand (Nonin Medical Inc., 8600FO MRI, Plymouth, MN). Breathing depth and frequency were recorded using an MRI-compatible respiratory belt (Siemens, Pi-Products, Amberg, Germany). Two self-adhesive electrodes were position over the muscle belly of the right forearm flexor, and sub-motor threshold was determined as previously mentioned. Electrical stimulation was delivered as symmetrical biphasic square waves using a portable stimulator that was modified for MRI compatibility. Stimulation settings remained consistent at 100Hz and 50μs. Prior to the HG protocol, participants performed two MVCs, and the higher of the two contractions was calibrated as 100%. All data were stored for later analysis (PowerLab, ADInstruments, Colorado Springs, CO).

3.4.2. Neuroimaging Recording

MRI data were collected using a 3-Tesla MRI (Magnetom TRIO TIM, Siemens Medical Solutions, Erlangen, Germany) with a 32-channel head coil. Anatomical scans were performed at the beginning of each scanning session using a high-resolution T1-weighted 3D MPRAGE sequence (sagittal, matrix 256x256mm, voxel size 1x1x1mm, 1mm slice thickness, no gap, flip angle 9°, TR 2.5ms, TE=2.98ms). Whole brain blood oxygen level-dependent (BOLD) contrast functional imaging data were acquired by means of a T2*-weighted gradient echo planar imaging (EPI) under the following

parameters: TE=30ms; flip angle=90°; field of view (FOV)=240x240mm; in-plane voxel resolution=3x3mm. Forty-five interleaved axial slices were acquired in each volume with a time-to-repetition (TR) of 2500ms. For each HG and HG+STIM trial, 248 volumes were acquired, while 132 volumes were acquired during the STIM trials.

3.4.3. Neuroimaging Data Analysis

Raw fMRI data were analyzed using Brain Voyager (Brain Innovation, The Netherlands). The first two images from each run were automatically discarded from the analysis due to magnetization equilibrium. Any functional scans demonstrating >2mm of movement were corrected with motion parameters, and then all functional scans were co-registered with the corresponding structural image.

Two levels of analysis were performed. First, individual design matrices were constructed for each time-course modeled by a boxcar and convolved with a canonical hemodynamic response function. In a second design matrix, the cortical activities of the HG protocols were correlated with a HR response using a HR regressor. For each participant, an average HR response for each HG protocol was calculated using 2.5s bins of HR data from an entire run. Individual participant regressors were then averaged into one HR regressor that was entered into analysis. The General Linear Model was used to create statistical parametric mapping on a voxel-by-voxel basis (Friston, et al. 1995). Second, the average contrast images from each individual representing the HG, STIM and HG+STIM protocols were separately

entered into a random effects group analysis. Finally, a t-test was performed to compare the average BOLD signal between HG and HG+STIM to determine regions that demonstrated more or less activation. Significant changes in signal intensity were determined for all paradigms.

BOLD responses compared to rest for all HG trials were corrected for multiple comparisons [false discovery rate (FDR), $p<0.05$] and a more lenient threshold of $p<0.05$, uncorrected, was used for STIM trials. A minimum cluster size of 20 voxels was used.

3.4.4. A Priori Regions of Interest

Our regions of interest were chosen based on previous data relating cortical structures to somatosensory stimulation and isometric HG exercise. Specifically, in human fMRI studies, the insula has been shown to process somatosensory information during painful and non-painful stimulations (Arienzo, et al., 2006) (Goswami, Frances, & Shoemaker, 2010). The anterior cingulate cortex (ACC) also demonstrates somatotopic sensory organization during similar nerve stimulation (Arienzo, et al., 2006). Previous somatosensory stimulation has also correlated an increase in HF-HRV within the ventral medial prefrontal cortex (vMPFC) (Goswami, Frances, & Shoemaker, 2010). Moderate intensity isometric HG exercise demonstrated bilateral ACC and insular activation (Wong, Masse, Kimmerly, Menon, & Shoemaker, 2007b), and decreased activity in the vMPFC and posterior cingulate cortex (PCC) (Wong, Masse, Kimmerly, Menon, & Shoemaker, 2007b). Therefore,

our *a priori* areas of interest and analysis consisted of the ACC, insula, and ventral medial prefrontal cortex.

CHAPTER 4 – RESULTS

4.1 Physiological Results

4.1.1. Heart Rate (HR)

During both laboratory (LAB) and MRI recording sessions, HR did not change during STIM compared to rest (Table 4. 1). HR increased above resting values in response to 30%HG, and progressively at each intensity level thereafter ($p<0.001$) (Table 4. 1). The respective average Borg ratings for HG at 30, 40, and 50% MVC were 11±2, 12±2, and 14±2, corresponding with light to somewhat hard exercise. There was a main effect of HG intensity on Borg scale values ($p<0.0001$), and force output ($p<0.0001$). There were no differences between HG and HG+STIM when comparing Borg scale values ($p=0.16$) and force output ($p=0.22$). These data suggest fatigue was not an issue between handgrip conditions. During the MRI session, HR increased from rest in response to HG (Table 4. 1) with a Borg rating of 11±3, corresponding with a light intensity exercise. However, during both LAB and MRI sessions, there were no differences in the HR change between HG and HG+STIM (Table 4. 1).

4.1.2. Heart Rate Variability

Unlike HR, high frequency (HF) HRV increased during STIM compared to rest during both LAB and MRI sessions (Figure 4. 1). In contrast, HF-HRV was decreased at all HG intensities during the LAB session (Figure 4. 2). This response was repeated during the MRI session where HF-HRV decreased from 4.26±0.7 during rest to 3.98±0.6 during 40%HG ($p<0.01$). Interestingly, during both recording sessions, the

effects of HG on HF-HRV were reversed during HG+STIM (LAB, Figure 4. 2) (MRI, Figure 4. 3).

Table 4. 1: Heart rate during LAB and MRI recording sessions in response to HG and HG+STIM at 30, 40, and 50% MVC, and STIM.

Average Rest	STIM			HG		HG+STIM	
HR (bpm)	HR (bpm)	ΔHR (bpm)		HR (bpm)	ΔHR (bpm)	HR (bpm)	ΔHR (bpm)
LAB							
59±7	58±6	1±1					
62±7			30%	64±7	2±3	65±6	3±3
63±7			40%	69±9*	6±6	72±8*	8±7
62±7			50%	76±11*	14±10	79±10*	17±9
MRI							
60±5	60±6	0±1					
61±4			40%	69±8*	8±5	71±11*	10±8

* $p<0.001$ significantly different from rest.
There was a main effect intensity during HG and HG+STIM on HR
(HG, handgrip; STIM, sub-motor somatosensory stimulation; HR, heart rate; ΔHR, delta heart rate; bpm, beats per minute)

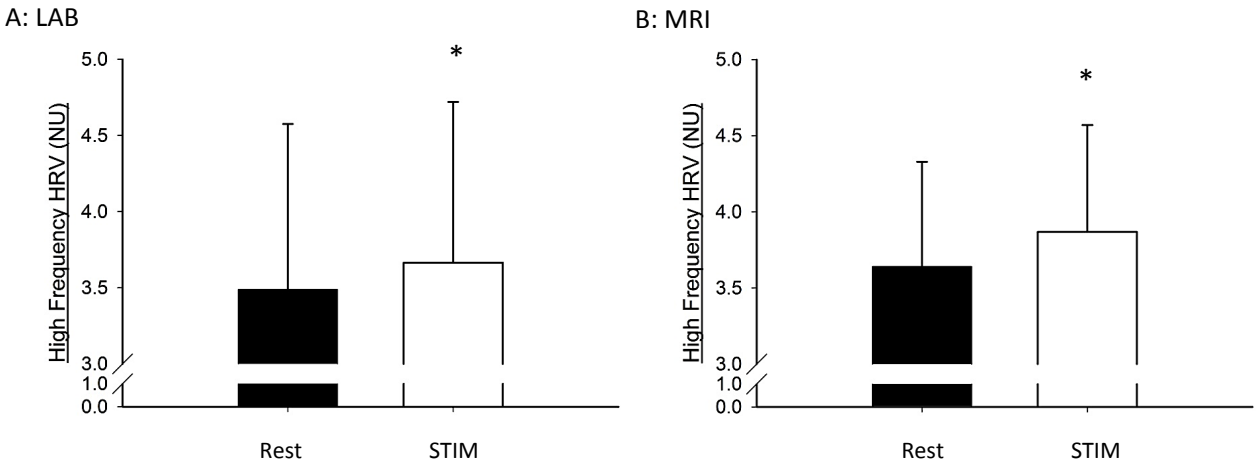

Figure 4. 1: HF-HRV during rest and STIM during the LAB and MRI recording sessions. STIM, sub-motor somatosensory stimulation; HF, high frequency; HRV, heart rate variability; NU, normalized units. *p<0.01.

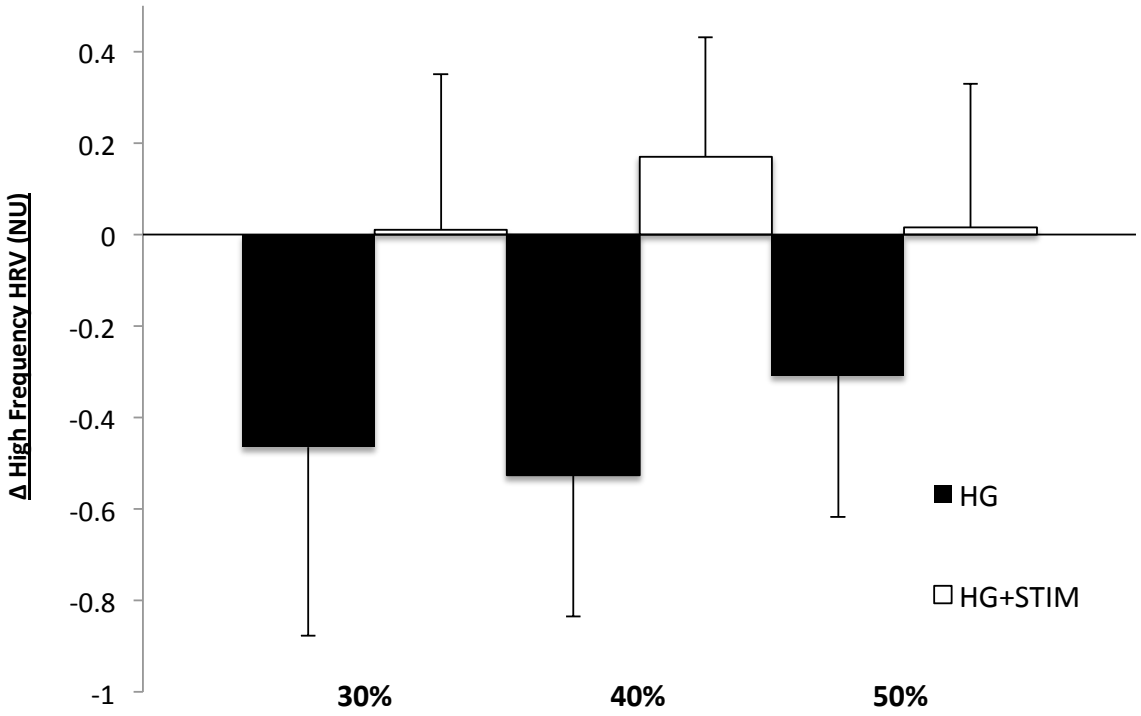

Figure 4. 2: Changes in HF-HRV in response to HG at 30, 40, and 50% MVC, with and without STIM. There was a main effect of condition on HRV ($p<0.01$). HG, handgrip; HG+STIM, handgrip+sub-motor somatosensory stimulation; HF, high frequency; HRV, heart rate variability; NU, normalized units.

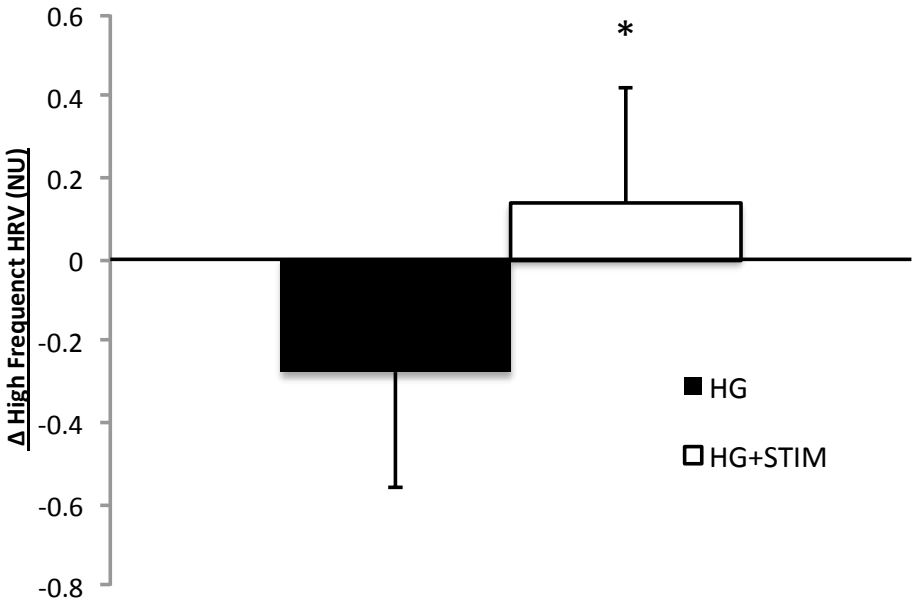

Figure 4. 3: Change in HF-HRV in response to 40%HG, with and without STIM during MRI session. HG, handgrip; HG+STIM, handgrip+sub-motor somatosensory stimulation; HF, high frequency; HRV, heart rate variability; NU, normalized units. *p<0.005.

4.2. Neuroimaging Results

4.2.1. Global Responses Correlated with the HG Task

4.2.1.1. Handgrip (HG)

In the overall global response, HG exercise was associated with increased activation, relative to rest, in the bilateral anterior insula (Figure 4. ; Table 4. 2), right mid insula, and right mid cingulate cortex (MCC) (Table 4. 2). Additional regions of increased activation included right primary motor cortex (M1; T-value 7.77) (Figure 4. 7), bilateral supplementary motor cortex (SMA; T-value R: 6.41; L: 5.73), right primary somatosensory cortex (S1; T-value 7.66), and right thalamus (T-value 5.11). Regions of deactivation, relative to rest, included the vMPFC (Figure 4. 4; Table 4. 2), right subgenual ACC, and left posterior cingulate cortex (PCC) (Table 4. 2).

4.2.1.2. HG+STIM

During HG+STIM, brain regions that displayed increased activity, relative to rest, included the right M1 (T-value 7.62) (Figure 4. 8), right S1 (T-value 7.29), and right thalamus (T-value 5.31). Regions demonstrating decreased neural activity, relative to rest, during HG+STIM were the vMPFC (T-value -5.10) (Figure 4. 5), and the left PCC (T-value -5.89).

4.2.1.3. Sub-motor Somatosensory Stimulation (STIM)

In response to STIM, there was increased activity, relative to rest, in the subgenual ACC, left posterior insula (Figure 4. 6; Table 4. 3), left mid insula, and right PCC ($p<0.05$, uncorrected) (Table 4. 3). Other areas included the bilateral caudate (L: 2.51; R: 4.69), bilateral cerebellum (L: 2.84; R: 2.64), and bilateral SMA (L: 2.69; R:

2.56). Areas of decreased activity, relative to rest, during STIM were vMPFC (Figure 4.6; Table 4. 3) and right thalamus (T-value -4.83) ($p<0.05$, uncorrected).

Table 4. 2: Brain region activations correlated to the 40% HG task.

Region	Side	Coordinates			T-score
		x	*y*	*z*	
A. Increased activity during 40%HG					
Anterior	R	32	13	11	5.19
Insula	L	-33	14	13	5.06
Mid Insula	R	35	-3	11	6.65
Mid CC	R	1	-5	38	5.57
B. Decreased activity during 40%HG					
vMPFC		-6	35	2	-5.19
Subgenual ACC		5	25	0	-5.14
PCC	L	-3	-57	18	-5.65

$p<0.05$, FDR corrected.
(PCC, posterior cingulate cortex; ACC, anterior cingulate cortex; vMPFC, ventral medial prefrontal cortex; R, right; L, left; HG, handgrip)

Table 4. 3: Brain regions correlated to the STIM task.

Region	Side	Coordinates			T-score
		x	*y*	*z*	
A. Increased activity during STIM					
Posterior Insula	L	-37	-20	9	2.83
Mid Insula	L	-35	-5	18	2.43
PCC	R	8	-42	12	4.92
Subgenual ACC		2	25	5	2.67
B. Decreased activity during STIM					
vMPFC		0	39	4	-2.56

$p<0.05$, uncorrected.
(vMPFC, ventral medial prefrontal cortex; ACC, anterior cingulate cortex; PCC, posterior cingulate cortex; R, right; L, left; STIM, sub-motor somatosensory stimulation)

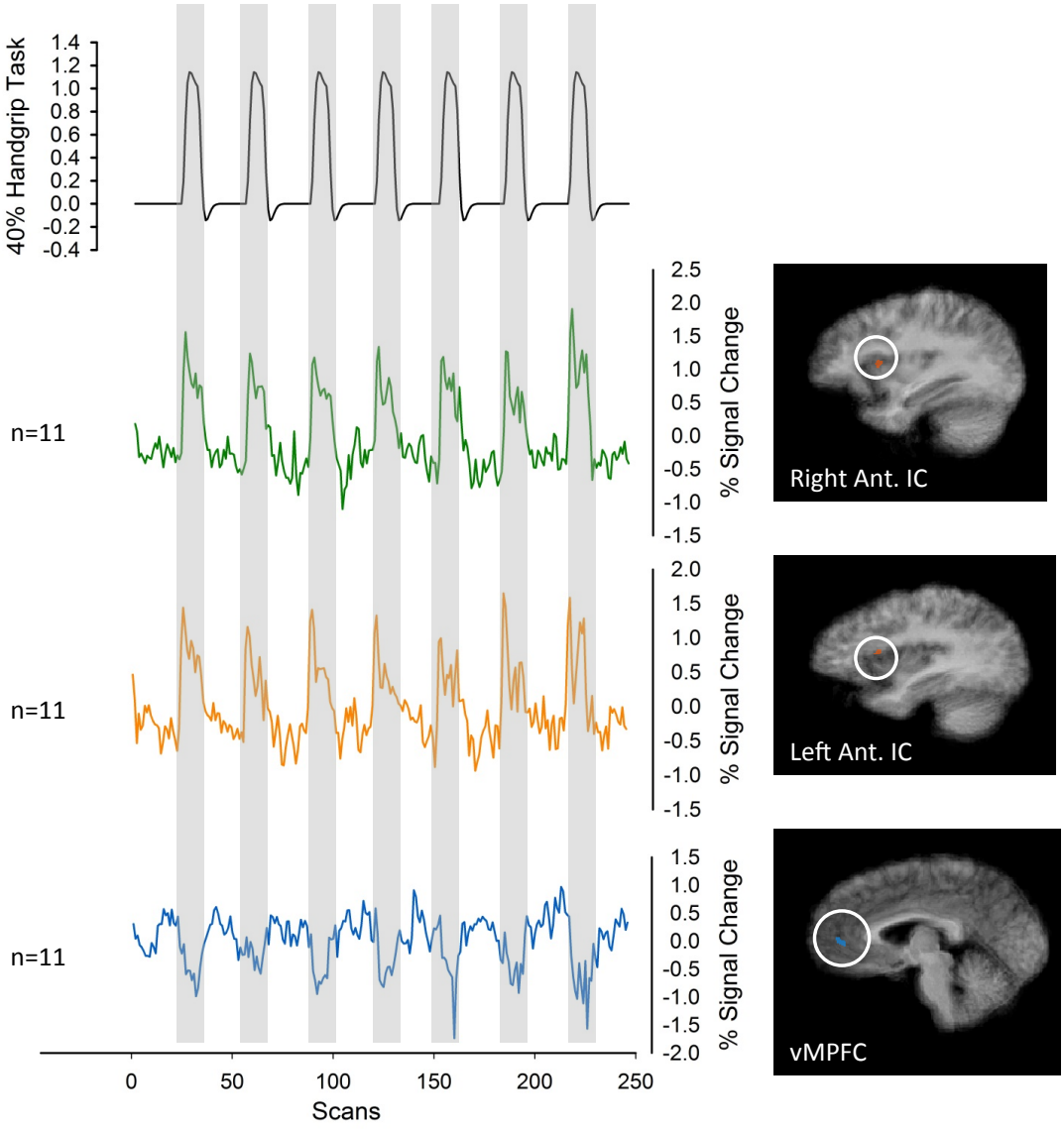

Figure 4. 4: Cortical activity in the bilateral anterior insula (Ant. IC) and ventral medial prefrontal cortex (vMPFC) correlated with the 40%handgrip task. n, number of participants with activation.

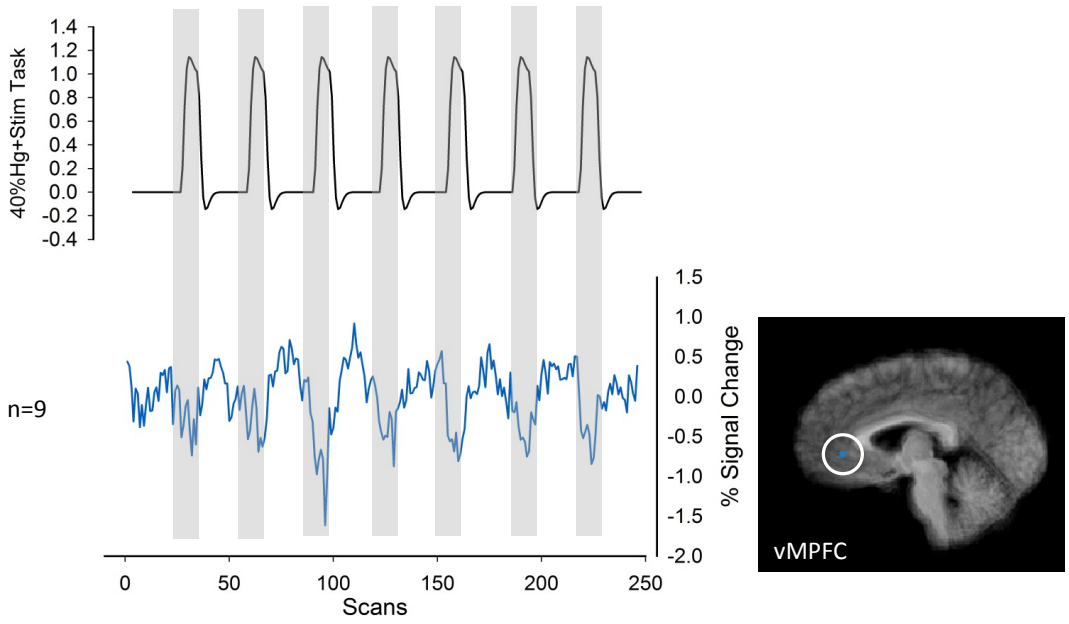

Figure 4. 5: Deactivation of the ventral medial prefrontal cortex (vMPFC) correlated with the 40%HG+STIM task. n, number of participants with activation; HG, handgrip; STIM, sub-motor somatosensory stimulation.

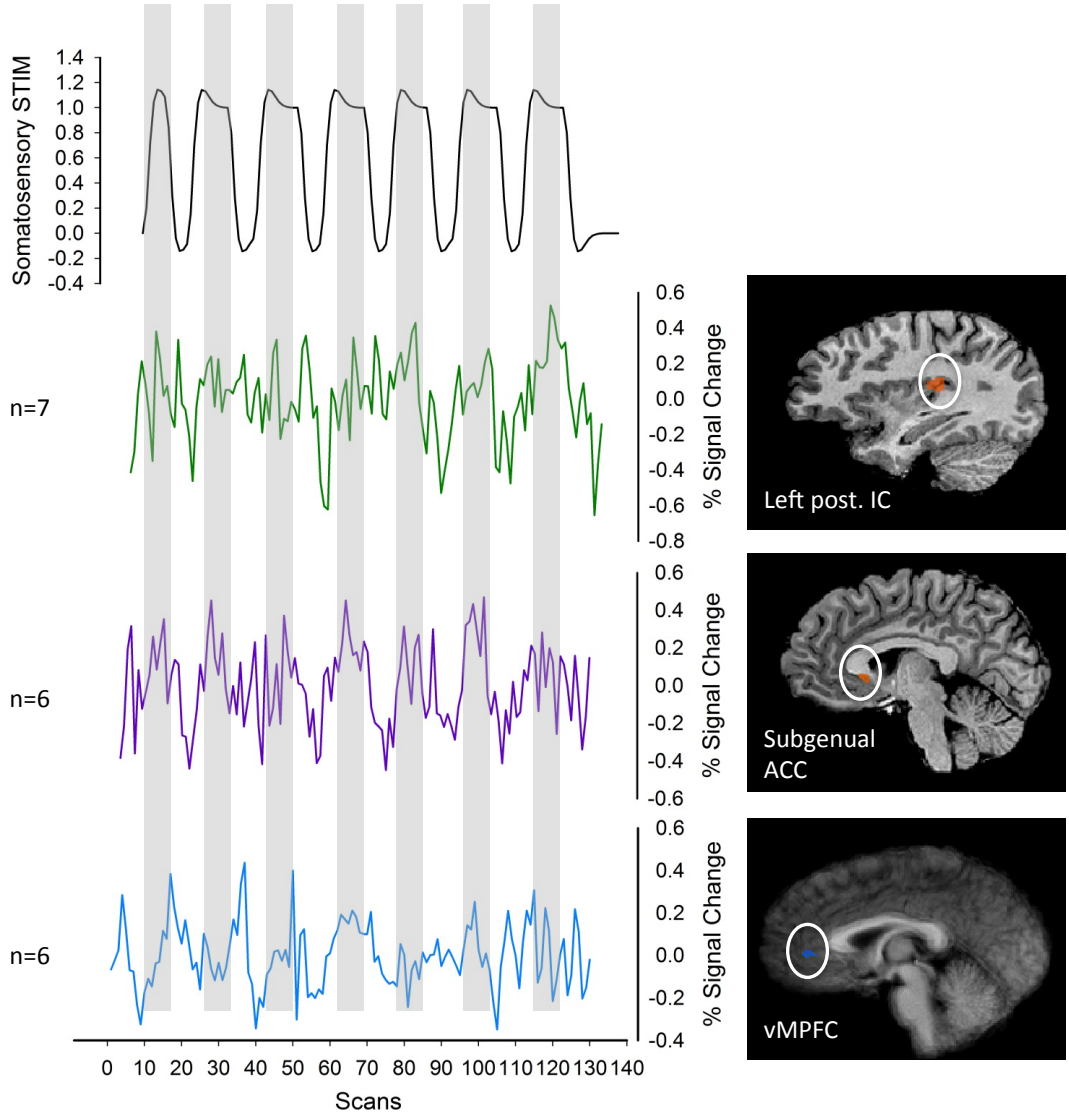

Figure 4. 6: Cortical activity in the posterior insula (PIC), subgenual anterior cingulate cortex (ACC), and ventral medial prefrontal cortex (vMPFC) correlated with the STIM task. STIM, sub-motor somatosensory stimulation; n, number of participants with activation.

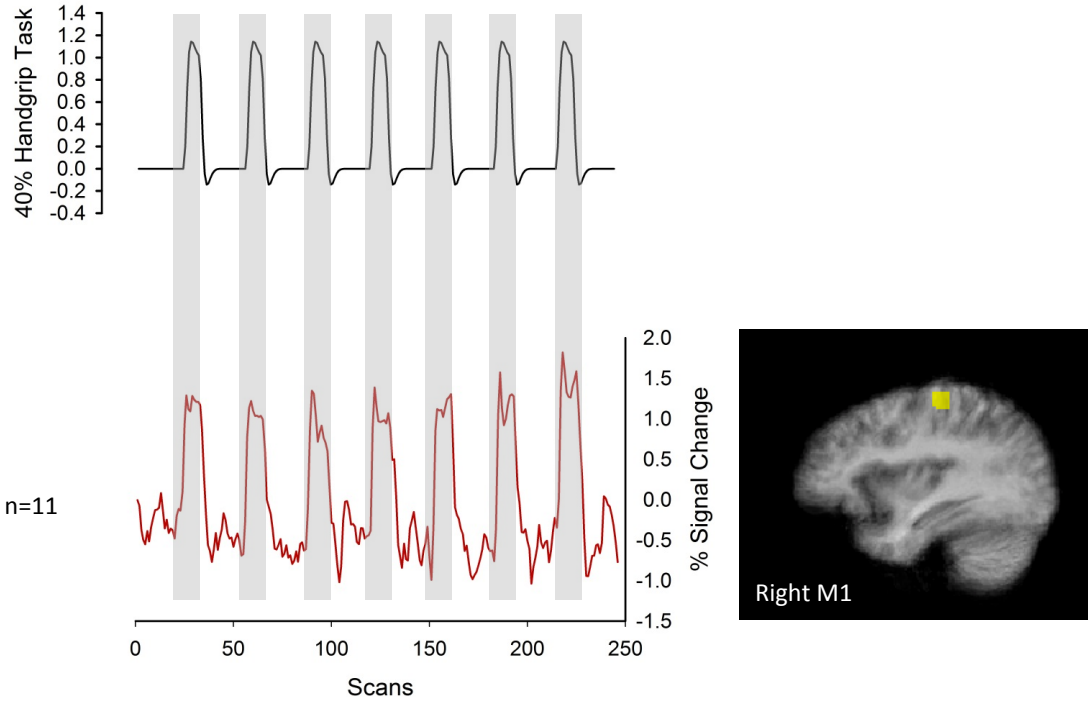

Figure 4. 7: Activation of M1 correlated with the 40%HG task. n, number of participants with activation; M1, primary motor cortex.

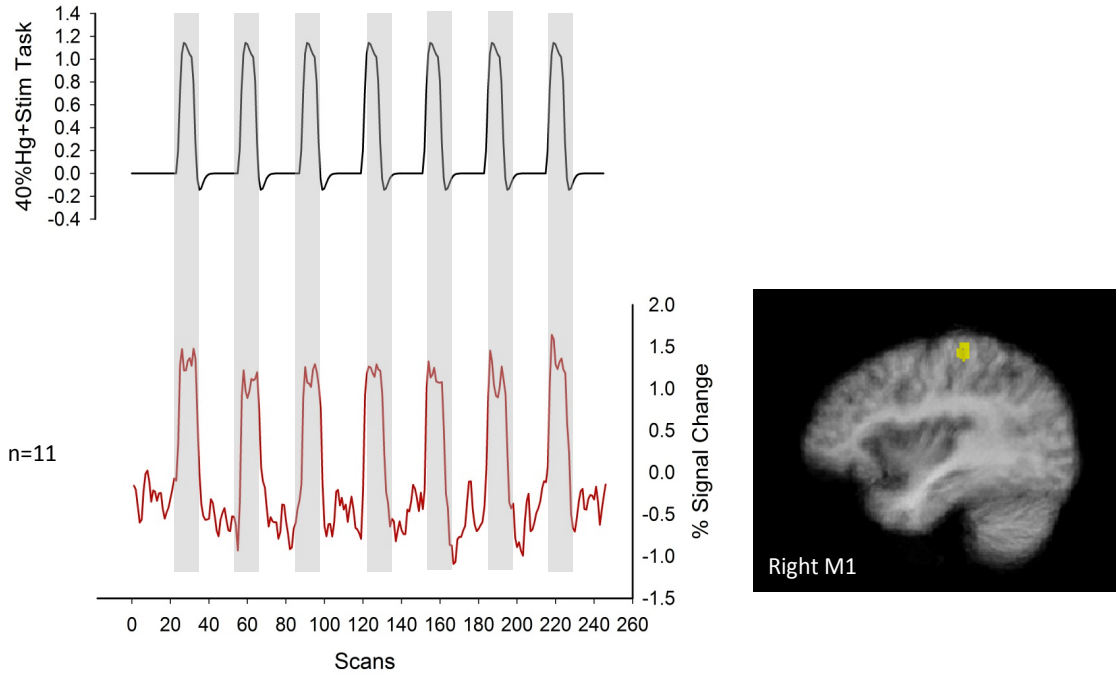

Figure 4. 8: Activation of M1 correlated with the 40%HG+STIM task. n, number of participants with activation; M1, primary motor cortex; HG, handgrip; STIM, sub-motor somatosensory stimulation.

4.2.2. Global Responses Correlated with the HR Response

4.2.2.1. Handgrip (HG)

The results of the global analysis during HG exercise reveal increased activation, relative to rest, of the bilateral anterior insular cortex (Figure 4. 9; Table 4. 4), bilateral mid insular cortex, and right posterior insular cortex ($p<0.05$, corrected) (Table 4. 4). In addition, other areas commonly observed were bilateral SMA (T-value right: 4.75; left: 4.81), right M1 (T-value 8.73), bilateral MCC (T-value right: 4.65, left: 4.95), right S1 (T-value 8.63), right thalamus (T-value: 5.61), right putamen (T-value: 4.68), and left cerebellum (T-value 4.73) ($p<0.05$, corrected). In addition there was common deactivation, relative to rest, within the vMPFC (Figure 4. 9; Table 4. 4), and right subgenual ACC ($p<0.05$, corrected) (Table 4. 4).

4.2.2.2. HG+STIM

Overall, less cortical activation was observed during HG+STIM compared with HG alone. During HG+STIM brain regions that demonstrated increased activity included the right M1, right S1, and right SMA ($p<0.05$, corrected) (Table 4. 5). Similar to the HG exercise, the vMPFC demonstrated decreased neural activity ($p<0.05$, corrected) (Figure 4. 10; Table 4. 5).

4.2.2.3. Sub-motor Somatosensory Stimulation (STIM)

Sub-motor somatosensory stimulation had no effect on heart rate. Therefore, there were no cortical patterns correlated with the HR response (Figure 4. 11).

Table 4. 4: Brain regions correlated to HR during 40%HG.

Region	Side	Coordinates			T-score
		x	*y*	*z*	
A. Increased activation during 40%HG					
Anterior Insula	R	36	18	9	4.74
	L	-32	13	12	5.30
Mid Insula	R	39	-4	11	6.88
	L	-38	-6	15	6.22
Posterior Insula	R	38	-25	17	4.49
B. Decreased activation during 40%HG					
vMPFC		5	33	-3	-5.33
Subgenual ACC	R	5	26	4	-4.50

$p<0.05$, FDR corrected.
(vMPFC, ventral medial prefrontal cortex; ACC, anterior cingulate cortex; R, right; L, left; HG, handgrip)

Table 4. 5: Brain regions correlated to HR during 40%HG+STIM.

Region	Side	Coordinates			T-score
		x	y	z	
A. Increased activation during 40%HG+STIM					
M1	R	36	-24	55	7.76
S1	R	29	-31	55	8.13
SMA	R	45	-2	33	6.65
B. Decreased activation during 40%HG+STIM					
vMPFC		-4	40	3	-8.24

p<0.05, FDR corrected.
(M1, primary motor cortex; S1, primary somatosensory cortex; SMA, supplementary motor area; vMPFC, ventral medial prefrontal cortex; R, right; L, left; HG+STIM, handgrip+sub-motor somatosensory stimulation)

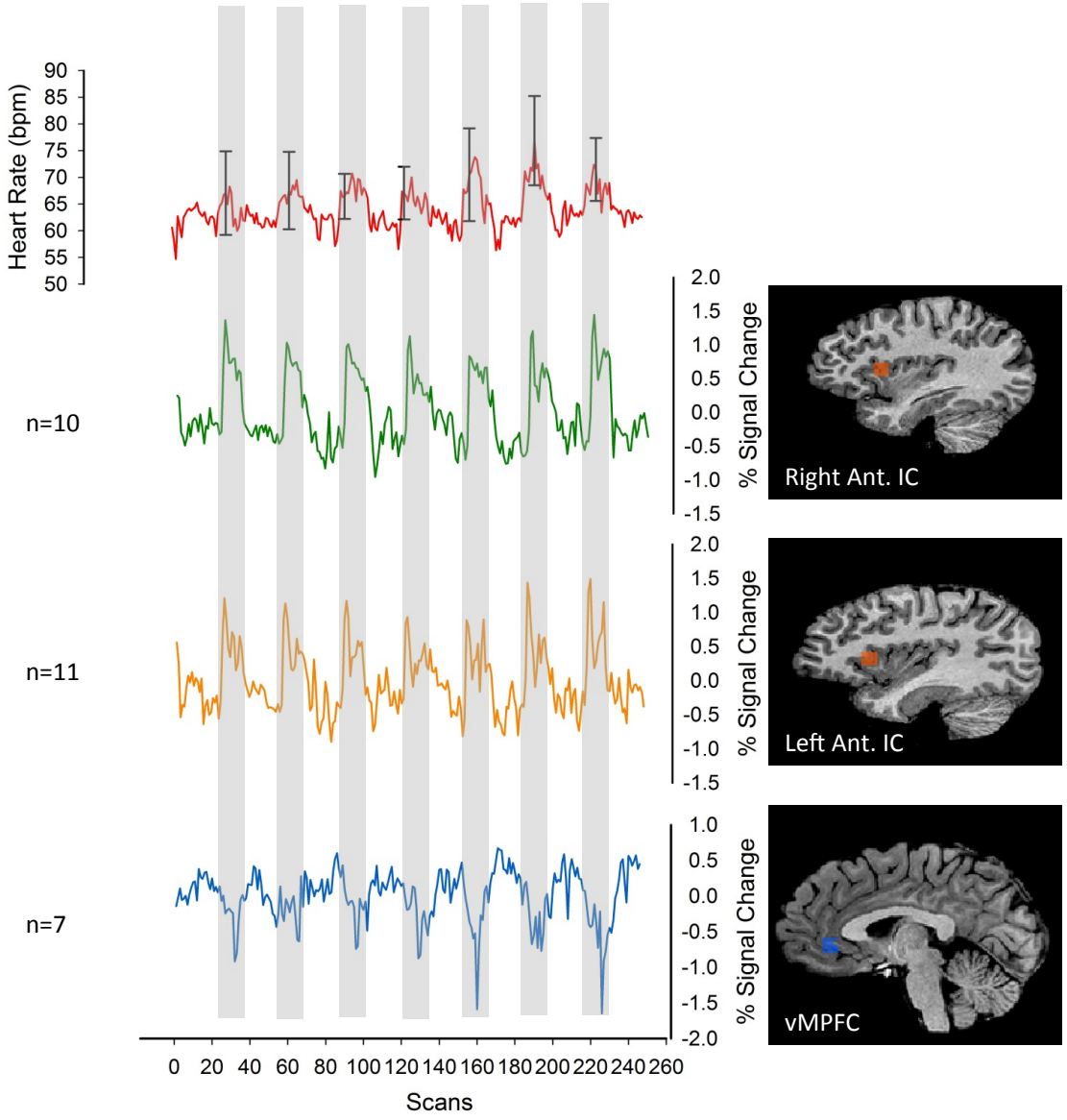

Figure 4.9: Activation patterns of the bilateral anterior insula (Ant. IC) and ventral medial prefrontal cortex (vMPFC) correlated with the heart rate response to 40%handgrip. n, number of participants with activation.

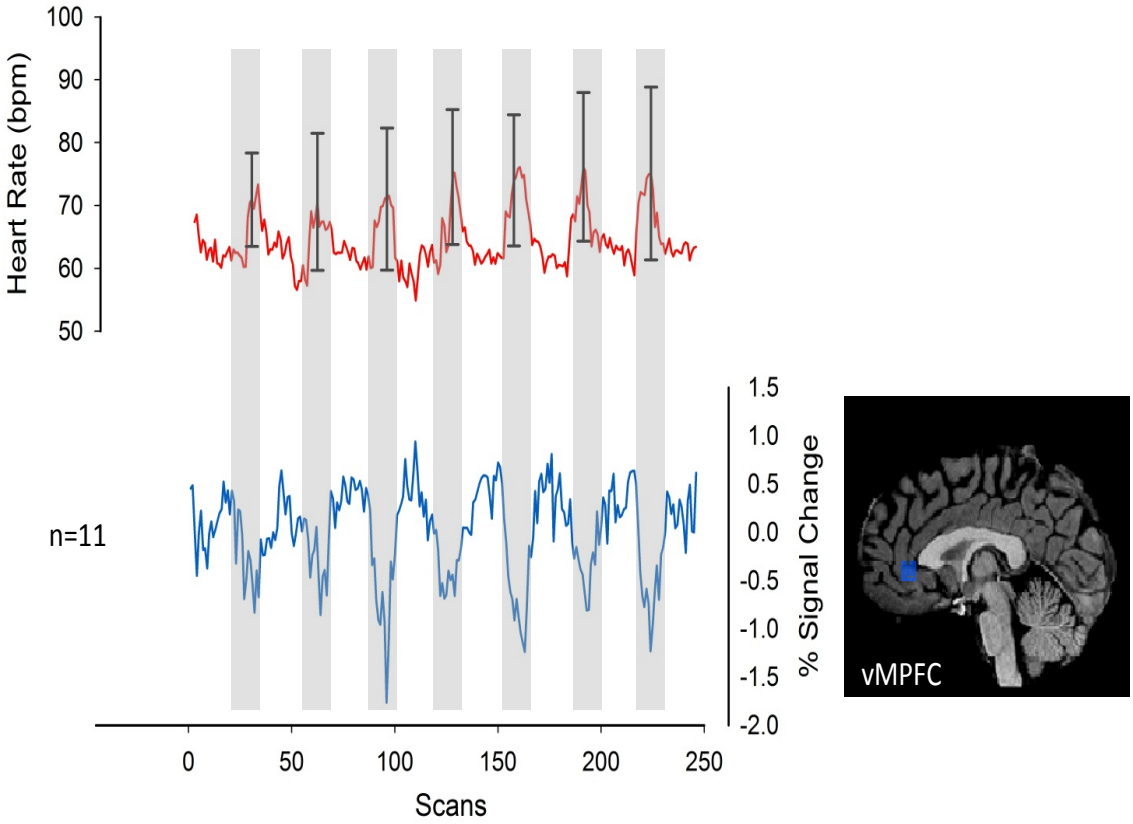

Figure 4. 10: Deactivation of the ventral medial prefrontal cortex (vMPFC) correlated with the heart rate response to 40%HG+STIM. n, number of participants with activation.

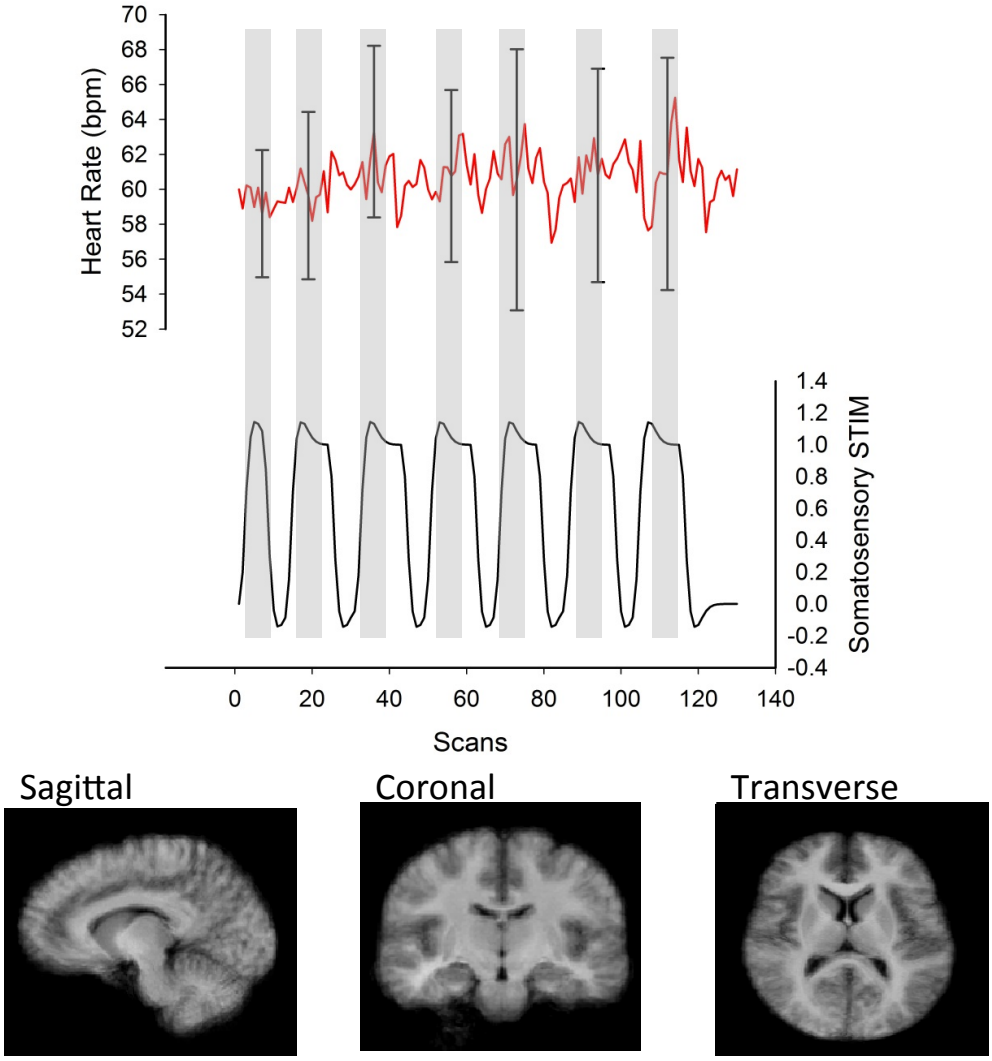

Figure 4. 11: Sub-motor somatosensory stimulation (STIM) had no effect on heart rate. Therefore, there were no cortical patterns correlated with the heart rate response.

4.2.3. Comparisons between HG and HG+STIM-induced changes in the BOLD Signal Response

A direct statistical comparison between HG and HG+STIM revealed greater deactivation in the vMPFC, subgenual ACC (Figure 4. 12), and bilateral putamen during HG versus HG+STIM (Table 4. 6). In addition, the vMPFC continued to demonstrate greater deactivation during HG versus HG+STIM at more conservative statistical thresholds (Table 4. 6). In contrast, no cortical regions showed greater activation during HG relative to HG+STIM.

Table 4. 6: Brain region activity during contrast of HG and HG+STIM.

Region	Side	Coordinates			T-score
		x	*y*	*z*	
More deactivation during HG>HG+STIM					
vMPFC		-2	37	0	-2.48 -3.27* -3.56**
Subgenual ACC		0	27	2	-2.26
Putamen	R	21	3	6	-2.27
	L	-25	2	4	-2.28

p<0.05, uncorrected.
*p<0.01, uncorrected.
**p<0.005, uncorrected.
(vMPFC, ventral medial prefrontal cortex; ACC, anterior cingulate cortex; R, right; L, left; HG, handgrip; HG+STIM, handgrip+sub-motor somatosensory stimulation)

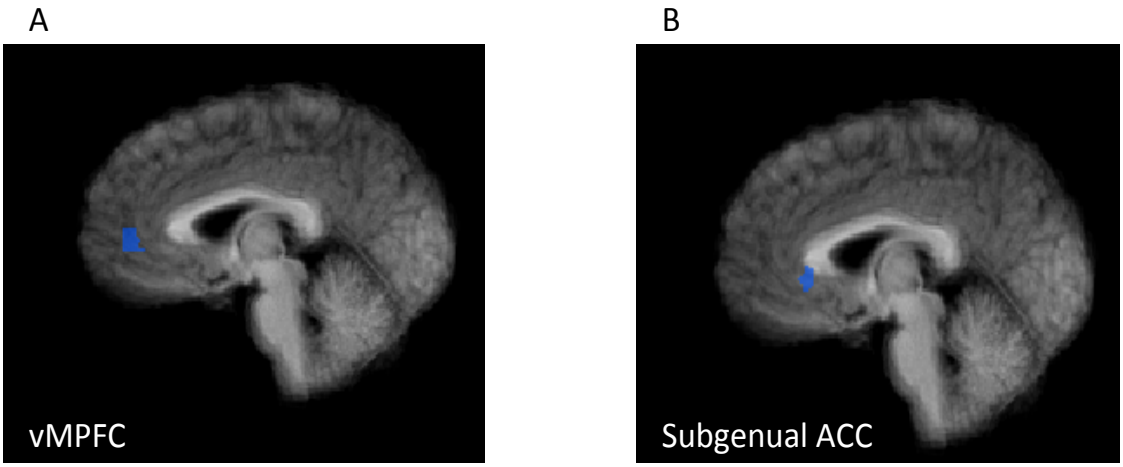

Figure 4. 12: Statistical comparison of the BOLD signal response between HG and HG+STIM. A: demonstrates greater deactivation in the ventral medial prefrontal cortex (vMPFC) during 40%HG versus 40%HG+STIM. B: demonstrates greater deactivation in the subgenual anterior cingulate cortex (ACC) during 40%HG versus 40%HG+STIM.

4.2.4. Cortical Region Signal Change during HG, STIM, and HG+STIM

The group average effect size of the BOLD signal in the vMPFC during STIM, HG, and HG+STIM are present in Figure 4. 13A. During 40% HG, the group average effect sizes for the left and right anterior insula were 0.19 and 0.23, respectively (Figure 4. 13B, C). During STIM, decreased activation, relative to rest, was observed in the vMPFC, whereas increased activation, relative to rest, was seen in the subgenual ACC and posterior insula cortex (Figure 4. 13D).

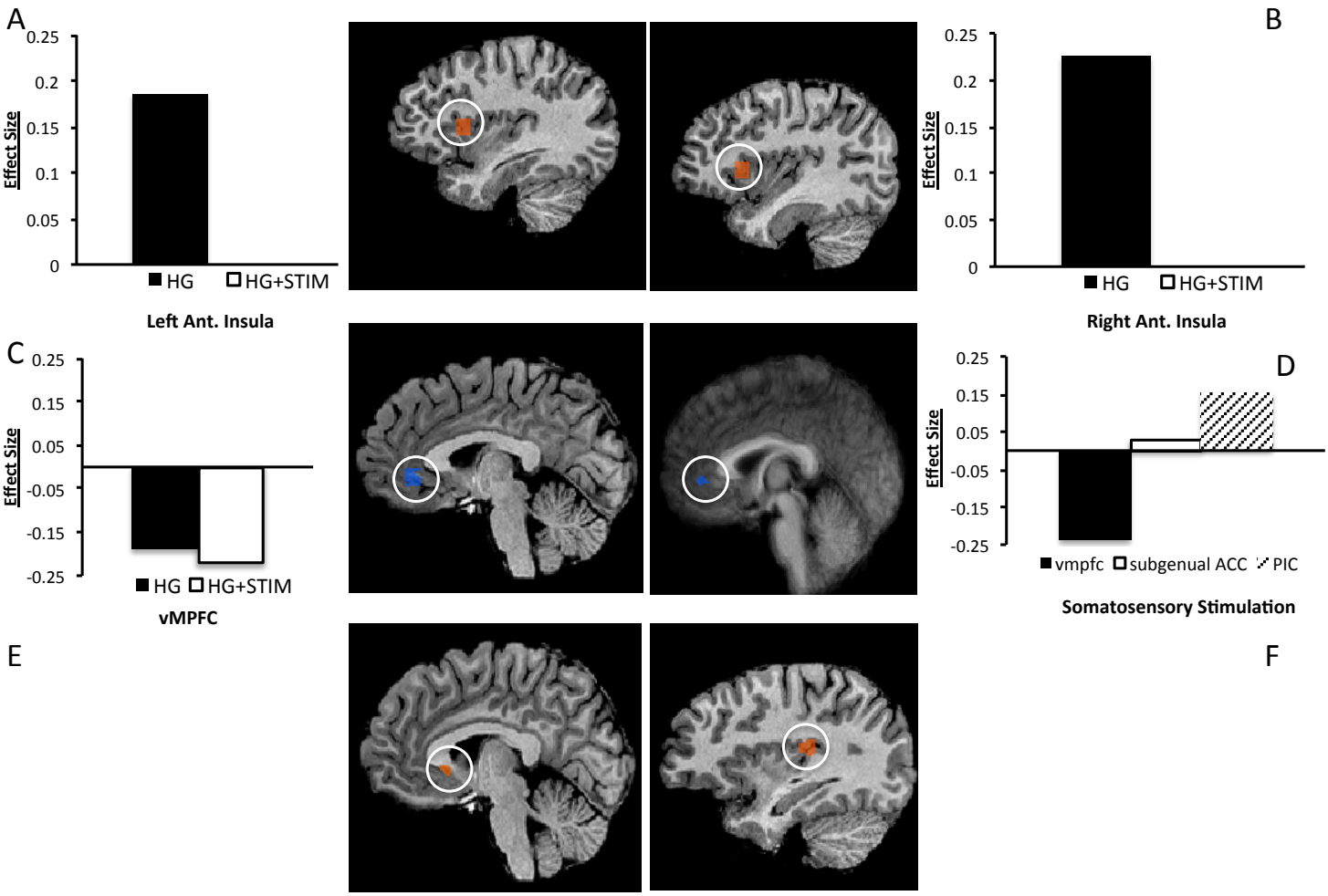

Figure 4. 13: A: Effect sizes of the left anterior insula during 40%HG and 40%HG+STIM. B: Effect sizes of the right anterior insula during 40%HG and 40%HG+STIM. C: Effect sizes of the vMPFC during 40%HG, 40%HG+STIM. D: Effect sizes of the vMPFC, subgenual ACC, and posterior insula cortex during STIM. E: Activation of the subgenual ACC. F. Increased activation of the posterior insula. HG, handgrip; STIM, somatosensory stimulation; vMPFC, ventral medial prefrontal cortex; ACC, anterior cingulate cortex; PIC, posterior insula cortex; ANT, anterior.

CHAPTER 5 – DISCUSSION

In this study, we demonstrated two important findings. First, STIM can reverse the changes in HF-HRV induced by HG exercise, and second, there is dissociation between HR and HF-HRV in response to STIM. The data suggest a view that activation of Type I and II fibers by STIM can modulate descending motor signals activated by HG exercise at the insula, and subsequently affect HF-HRV. STIM alone resulted in posterior insular activation and increased HF-HRV. HG alone increased activity within the anterior insular cortex, reduced activity within the vMPFC, and reduced HF-HRV. However, when HG was performed concurrently with STIM, anterior insular activation was no longer evident, and the effects on HF-HRV were reversed. Lastly, despite our hypothesis, STIM had no effect on HR at rest or in response to HG. Therefore, it appears that the somatosensory information affects HRV and not HR pointing to enhanced complexity of autonomic cardiovascular control. In support of this, vMPFC deactivation and HR responses remained consistent during both HG and HG+STIM. Overall, in support of the hypothesis, the current results suggest STIM can modulate the HF-HRV changes induced by HG but not the HR itself. Furthermore, differences in cortical activation patterns suggest these changes are reflected within the CAN.

5.1. vMPFC

The results agree with previous research that has highlighted the vMPFC as a key cortical structure in HR regulation. During both HG and HG+STIM, there was

similar deactivation within the vMPFC, as well as similar HR responses, during the two HG conditions. Anatomically, the MPFC has major projections to subcortical autonomic structures, which can all affect HR regulation. The MPFC projects to the hypothalamus and periaqueductal grey (An, Bandler, Ongur, & Price, 1998; Ongur, An, & Price, 1998), and the ventral subdivision of the MPFC projects directly to the nucleus tractus solitarius (Owens & Verberne, 1996) and the dorsal motor nucleus of the vagus (Blessing, Li, & Wesselingh, 1991). In animals, electrical stimulation of various areas of the MPFC reveals depressor sites within the ventral subdivision (Verberne, 1996; Owens NC & Verberne, 2001; Fisk & Wyss, 1997), which when stimulated, produce corresponding decreases in HR (Fisk & Wyss, 1997; Owens NC and Verberne, 2001). In humans, the level of MPFC activation regulates the HR response during baroreceptor unloading (Kimmerly, O'Leary, Menon, Gati, & Shoemaker, 2005). As well, Wong et al. (2007b) correlated the HR response to HG exercise with deactivation of the vMPFC (Wong, Masse, Kimmerly, Menon, & Shoemaker, 2007b). The above liteature supports a role of the vMPFC in HR control, which is congruent with our results.

5.2. Insular Cortex

The insular cortex has numerous connections with both cortical and subcortical structures. In primates, the insula has connections with the frontal, temporal, and parietal lobes, as well as the ACC (Augustine, 1996). In addition, the insula also projects directly to sub-cortical structures such as areas of the amygdala, brain stem and thalamus, which are all involved in autonomic control (Saper, 1982; Shipley,

1982; Shipley & Sanders, 1982). Based on its wide spread anatomical projections, the insula could play an instrumental role in autonomic function.

During various tasks such as HG (motor), emotional and mental stressors, and autonomic challenges, the insula has been linked with changes in HRV (Critchley, et al., 2003; Gianaros, Van der Veen, & Jennings, 2004; Macey, et al., 2012). Furthermore, clinical studies looking at the effects of an insular stroke have highlighted the insula as a key autonomic structure in HRV regulation (Naver, Blomstrand, & Wallin, 1996; Oppenheimer, Kedem, & Martin, 1996; Colivicchi, Bassi, Santini, & Caltagirone, 2004). Our results support the literature demonstrating a role of the insula cortex in HRV.

5.2.1. Anterior insular activation during volitional handgrip

The insular cortices have been recognized as having distinct functional regions, and our results revealed that during HG, there was increased activation of the bilateral anterior insular cortex, concurrent with a decrease in HF-HRV, and increase in HR, from rest. The anterior insula has projections to basal forebrain structures and brainstem nuclei, which play a major role in modulating autonomic function (Ongur & Price, 2000). In addition, numerous studies using isometric HG to alter cardiovascular variables such as HR and HRV, have reported increased activation within the insula (King, Menon, Hachinski, & Cechetto, 1999), and specifically the anterior insula cortex (Goswami, Frances, & Shoemaker, 2010; Wong, Masse, Kimmerly, Menon, & Shoemaker, 2007b). Furthermore, in agreement with our

results, Critchley et al., (2003) demonstrated bilateral insular activation associated with decreased HRV during HG exercise (Critchley, et al., 2003).

5.2.2. Posterior insular activation during somatosensory stimulation

During STIM there was increased activation, from rest, in the posterior insular cortex, and an increase in HF-HRV. Evidence in rats has implicated the insula to be viscerotopically organized for processing ascending somatosensory information (Cechetto & Saper, 1987). Subsequent neuroimaging studies have confirmed a similar arrangement in the human cortex (King, Menon, Hachinski, & Cechetto, 1999). In primates, the posterior insula interconnects with several somatosensory cortical areas, including a processing pathway that can be followed from the primary (SI) and secondary (SII) somatosensory cortices, through the insula (Friedman, Murray, O'Neill, & Mishkin, 1986). In addition, neuron recordings from the posterior insula reveal a large number of sites that respond to somatosensory stimulation of various body parts (Schneider, Friedman, & Mishkin, 1993). In humans, vibration of the hands and feet also causes bilateral increases in regional cerebral blood flow in the posterior insula (Burton, Videen, & Raichle, 1993). Meanwhile, fMRI studies reveal the insula is involved in processing somatosensory information during painful and non-painful stimulations (Arienzo, et al., 2006). Previous work in our laboratory also using STIM combined with functional imaging has revealed muscle afferent representation within the posterior insula cortex (Goswami, Frances, & Shoemaker, 2010).

5.2.3. Changes in cortical activation patterns during HG+STIM

When HG and STIM were combined, anterior insular activation was no longer evident, and the decrease in HF-HRV associated with HG was reversed. Our results lead us to speculate that activation of Type I and II fibers by STIM may modulate descending motor signals activated by HG exercise. Furthermore, based on the change in activation patterns, the insula may be a key cortical site for modulation. In support of this, Williamson et al., (1997) demonstrated insula cortex activation during active, but not passive, cycling. The authors suggested that during volitional exercise, a cortical site involved in central command might have activated the insula cortex, which in turn activated well-established areas of cardiovascular control (Williamson, et al., 1997). Based on our results, and those of Williamson et al. (1997), we speculate that activation of M1 during the HG exercise could play an important role in activating regions of the anterior insular cortex. In addition to cortical-cortical and cortical-subcortical connections, studies using horseradish peroxidase injections into the insula also revealed an abundance of local intra-insular connections (Friedman, Murray, O'Neill, & Mishkin, 1986). Therefore, we speculate that activation of the posterior insula via STIM may have inhibited the activation of the anterior insula via intra-insular projections, allowing the posterior insula to elicit its own influences on areas of cardiovascular control.

5.3. Other Areas associated with Somatosensory Stimulation

Other areas that were active during STIM included the caudate, PCC, SMA, and cerebellum. In primates, including humans, there are both afferent and efferent

connections between the insula and caudate (Augustine, 1985). Therefore it is conceivable that activation of the insula could elicit activation within the caudate. Secondly, the PCC has been functionally recognized as a part of a default network of brain function. The cortical structures within this network are usually active when the brain is in a resting state (Raichle, MacLeod, Snyder, Powers, Gusnard, & Shulman, 2001), a condition similar to our stimulation protocol. Activation of the SMA is congruent with other stimulation studies, which demonstrated somatotopic sensory organization within the SMA (Arienzo, et al., 2006). Therefore, activation of the SMA gives us confidence that our technique of somatosensory stimulation was detected by and represented within the brain. Finally, the cerebellum is often involved in motor paradigms and movement preplanning. However, the cerebellum has also been observed to be associated with increasing HF-HRV (Critchley, et al., 2003; Napadow, Dhond, Conti, Makris, Brown, & Barbieri, 2008), supporting its pattern of activation within the current study.

5.4. Assumptions/Limitations

An assumption of the current study was the involvement of sympathetic activity. We did not measure sympathetic activity, and therefore we do not know of any changes in sympathetic drive that may have been occurring throughout each protocol. However, based on previous research implementing short duration (<30s) isometric HG exercise and MSNA (Wong, et al. 2007b), we assumed sympathetic activation was not involved during the lower intensity HGs. Therefore, our main findings during HGs performed at lower intensity were under conditions of largely

parasympathetic withdrawal. However, this is not to say that sympathetic drive did not increase as HG intensity increased. Finally, we assumed we were targeting Type I and II sensory afferents during STIM. In spite of this assumption, based on our knowledge of muscle afferent recruitment patterns, larger diameter Type I/II fibers demonstrate less resistance to current flow, and therefore, are preferentially recruited at low stimulation intensities over smaller diameter Type III and IV's (Swett & Bourassa, 1981). A limitation of this study is the very liberal statistics for STIM. Despite the liberal statistic used to uncover the effect of STIM within the CAN, we are confident of our results as they coincide with previous work demonstrating similar regions of activation (Goswami, Frances, & Shoemaker, 2010). Our small sample size (n=11) would pose as another limitation to this study. It has been reported that an n of at least 20 should be used in neuroimaging studies in order to ensure reproducibility (Thirion, Pinel, Meriaux, Roche, Dehaene, & Poline, 2007). However, by applying very conservation thresholds to the HG and HG+STIM protocols, we hoped to negate this limitation. At the same time, perhaps a larger sample size would have helped uncover the effects of STIM under more conservative statistical thresholds.

CHAPTER 6 – CONCLUSION

In summary, the present study used sub-motor electrical stimulation of the forearm muscle and handgrip exercise to analyze the effects of somatosensory signals on heart rate and heart rate variability at rest and during HG. In addition, functional

imaging was used to provide evidence of cortical patterns associated with each HG and STIM task on its own, and when combined. Our results support past literature highlighting the vMPFC and insular cortex in heart rate and heart rate variability regulation, respectively. However, our novel finding is dissociation between heart rate and heart rate variability regulation within the cortical autonomic network in a manner that was exposed by the STIM protocol. This finding is supported by a change in cortical activation patterns within the insula during HG versus HG+STIM. The lack of insular activation during HG+STIM, concurrent with a change in HF-HRV seen during HG alone, supports a role of the insula in heart rate variability regulation. Posterior insular activation during somatosensory stimulation supports previous literature highlighting this structure as a somatosensory processing area. However, it also leads us to speculate that performing somatosensory stimulation and HG exercise together may have exposed an inhibitory role between the posterior and anterior regions of the insula. As well, during HG, concurrent descending cortical signals and ascending signals from the active muscle appear to compete for control over HR. The current results indicate that such complex signal processing occurs within the CAN with separate impact on HR and HRV. Clearly, the addition of sensory inputs from a “resting” muscle during a volitional task performed by the contralateral arm upsets the normal outcome.

REFERENCES

Adreani, C., Hill, J., & Kaufman, M. (1997). Responses of group III and IV muscle afferents to dynamic exercise. *Journal of Applied Physiology , 82*, 1811-1817.

Akselrod, S., Gordon, D., Ubel, F., Shannon, D., Barger, A., & Cohen, R. (1981). Power spectrum analysis of heart rate fluctuation: a quantitative probe of beat-to-beat cardiovascular control. *Science , 213* (4504), 220-222.

Alam, M., & Smirk, F. (1937). Observations in man upon a blood pressure raising reflex arising from the voluntary muscles. *Journal of Phyiology , 89* (4), 372-383.

Alper, R., Jacob, H., & Brody, M. (1987). Regulation of arterial pressure lability in rats with chronic sinoaortic deafferentation. *American Journal of Physiology - Circulatory Physiology , 253*, H466-H474.

An, X., Bandler, R., Ongur, D., & Price, J. (1998). Prefrontal cortical projections to longitudinal columns in the midbrain periaqueductal gray in macaque monkeys. *The Journal of Comparative Neurology , 401*, 455-479.

Arienzo, D., Babiloni, C., Ferretti, A., Caulo, M., Del Gratta, C., Tartaro, A., et al. (2006). Somatotopy of anterior cingulate cortex (ACC) and supplementary motor area (SMA) for electrical stimulation of the median and tibial nerves: An fMRI study. *NeuroImage , 33*, 700-705.

Augustine, J. (1996). Circuitry and functional aspects of the insular lobe in primates including humans. *Brain Research Reviews , 22*, 229-244.

Augustine, J. (1985). The insular lobe in primates including humans. *Neurological Research , 7*, 2-10.

Billman, G. (2011). Heart rate variability - a historical perspective. *Frontiers in Physiology , 2* (86), 13.

Blessing, W., Li, Y., & Wesselingh, S. (1991). Transneuronal transport of the herpes simplex virus from the cervial vagus to brain neurons with axonal inputs to the central vagal sensory nuclei in the rat. *Neuroscience , 42* (1), 261-274.

Borg, G. (1982). Psychophysical bases of perceived exertion. *Medical & Science in Sport & Exercise , 14*, 377-381.

Borst, C., Hollander, A., & Bouman, L. (1972). Cardiac acceleration elicited by voluntary muscle contractions of minimal duration. *Journal of Applied Physiology , 32*, 70-77.

Brown, G., Perthen, J., Liu, T., & Buxton, R. (2007). A primer on functional magnetic resonance imaging. *Neuropsychol Rev , 17*, 107-125.

Burton, H., Videen, T., & Raichle, M. (1993). Tactile-vibration-activated foci in insular and parietal-opercular cortex studied with positron emission tomogaphy: Mapping the second somatosensory area in humans. *Somatosensory and Motor Research , 10* (3), 297-308.

Cechetto, D., & Saper, C. (1987). Evidence for a viscerotopic sensory representation in the cortex and thalamus in the rat. *Journal of Comparative Neurology , 262*, 27-45.

Chess, G., Tam, R., & Calaresu, F. (1975). Influence of cardiac neural inputs on rhythmic variations of heart period in the cat. *American Journal of Physiology , 228* (3), 775-780.

Coghill, R., Talbot, J., Evans, A., Meyer, E., Gjedde, A., Bushnell, C., et al. (1994). Distributed processing of pain and vibration by the human brain. *The Journal of Neuroscience , 14* (7), 4095-4108.

Cole, R., Blackstone, E., Pashkow, F., Snader, C., & Lauer, M. (1999). Heart-rate recovery immediately after exercise as a predictor of mortality. *New England Journal of Medicine , 341*, 1351-1357.

Colivicchi, F., Bassi, A., Santini, M., & Caltagirone, C. (2004). Cardiac autonomic derangement and arrhythmias in right-sided stroke with insular involvement. *Stroke , 35*, 2094-2098.

Critchley, H. (2004). The human cortex responds to an interoceptive challenge. *Proceedings of the National Academy of Science , 101* (17), 6333-6334.

Critchley, H., Corfield, D., Chandler, M., Mathias, C., & Dolan, R. (2000). Cerebral correlates of autonomic cardiovascular arousal: functional neuroimaging investigation in humans. *Journal of Physiology , 523* (1), 259-270.

Critchley, H., Mathias, C., Josephs, O., O'Doherty, J., Zanini, S., Dewar, B., et al. (2003). Human cingulate cortex and autonomic control: converging neuroimaging and clinical evidence. *Brain , 126*, 2139-2152.

Devinsky, O., Morrell, M., & Vogt, B. (1995). Contributions of anterior cingulate cortex to behaviour. *Brain , 118*, 279-306.

Fisk, G., & Wyss, J. (1997). Pressor and depressor sites are intermingled in the cingulate cortex of the rat. *Brain Research , 754*, 204-212.

Flynn, F., Benson, D., & Ardila, A. (1999). Anatomy of the insula - functional and clinical correlates. *Aphasiology , 13* (1), 55-78.

Friedman, D., Murray, E., O'Neill, J., & Mishkin, M. (1986). Cortical connections of the somatosensory fields of the lateral sulcus of macaques: evidence for a corticolimbic pathway for touch. *Journal of Comparative Neurology , 252* (3), 323-347.

Friston, K., Holmes, A., Worsley, K., Poline, J., Frith, C., & Frackowiak, R. (1995). Statistical parametric maps in functional imaging: a general linear approach. *Human Brain Mapping , 2*, 189-210.

Gademan, M., Sun, Y., Han, L., Valk, V., Schalij, M., van Exel, H., et al. (2011). Rehabilitation: Periodic somatosensory stimulation increases arterial baroreflex sensitivity in chronic heart failure patients. *International Journal of Cardiology , 152*, 237-241.

Gianaros, P., Van Der Veen, F., & Jennings, J. (2004). Regional cerebral blood flow correlates with heart period and high-frequency heart period variability during working-memory tasks: Implications for the cortical and subcortical regulation of cardiac autonomic activity. *Psychophysiology , 41*, 521-530.

Goswami, R., Frances, M., & Shoemaker, J. (2011). Representation of somatosensory inputs within the cortical autonomic network. *NeuroImage , 54*, 1211-1220.

Guyenet, P. (1990). *Role of the ventral medulla oblongata in blood pressure regulation.* (A. Loewy, & K. Spyer, Eds.) New York: Oxford University Press.

Hollman, J., & Morgan, B. (1997). Effect of transcutaneous electrical nerve stimulation on the pressor response to handgrip exercise. *Journal of the American Physical Therpay Association , 77*, 28-36.

Hurley, K., Herbert, H., Moga, M., & Saper, C. (1991). Efferent projections of the infralimbic cortex of the rat. *The Journal of Comparative Neurology , 308*, 249-276.

Jacobsson, F., Himmelmann, A., Bergbrant, A., Svensson, A., & Mannheimer, C. (2000). The effect of transcutaneous electric ner stimulation in patients with therapy-resistant hypertension. *Journal of Human Hypertension , 14*, 795-798.

Jose, A., & Collison, D. (1970). The normal range and determinants of the intrinsic heart rate in man. *Cardiovascular Research , 4*, 160-167.

Kaada, B. (1951). Somato-motor, autonomic and electrocorticogaphic responses to electrical stimulation of rhinencephalic and other structures in primates, cat, and dog; a study of responses from limbic, subcallosal, orbito-insular, piriform and temporal cortex, hippocampus-fornix and amygdala. *Acta Physiologica Scandinavica Supplementum , 24* (83), 1-262.

Kaada, B., Flatheim, E., & Woie, L. (1991). Low-frequency transcutaneous nerve stimulation in mild/moderate hypertension. *Clinical Physiology , 11*, 161-168.

Kaufman, M., & Hayes, S. (2002). The exercise pressor reflex. *Clinical Autonomic Research , 12*, 429-439.

Kaufman, M., Longhurst, J., Rybicki, K., Wallach, J., & Mitchell, J. (1983). Effects of static muscular contraction on impulse activity of group III and IV afferents in cats. *Journal of Applied Physiology , 55*, 105-112.

Kaufman, M., Rybicki, K., Waldrop, T., & Ordway, G. (1984). Effect of ischemia on responses of group III and IV afferents to contraction. *Journal of Applied Physiology , 57*, 644-650.

Kimmerly, D., O'Leary, D., Menon, R., Gati, J., & Shoemaker, J. (2005). Cortical regions associated with autonomic cardiovascular regulation during lower body negative pressure in humans. *Journal of Physiology , 569*, 331-345.

King, A., Menon, R., Hachinski, V., & Cechetto, D. (1999). Human forebrain activation by visceral stimuli. *The Journal of Comparative Neurology , 413*, 572-582.

Kleiger, R., Mille, J., Bigger, J. J., & Moss, A. (1987). Decrease heart rate variability and its association with increased mortality after acute myocardial infarction. *American Journal of Cardiology , 59*, 256-262.

Kurth, F., Eickhoff, S., Schleicher, A., Hoemke, L., Zilles, K., & Amunts, K. (2009). Cytoarchitecture and probabilistic maps of the human posterior insular cortex. *Cerebral Cortex , 20*, 1448-1461.

Lane, R., McRae, K., Reiman, E., Chen, K., Ahern, G., & Thayer, J. (2009). Neural correlates of heart rate variability during emotion. *NeuroImage , 44*, 213-222.

Lind, A., & McNicol, G. (1967). Circulatory responses to sustained hand-grip contractions performed during other exercise, both rhythmic and static. *Journal of Physiology , 192*, 595-607.

Lind, A., Taylor, S., Humphreys, P., Kennelly, B., & Donald, K. (1964). The circulatory effects of sustained voluntary muscle contraction. *Clinical Science , 27*, 229-244.

Loewy, A. (1981). Descending pathways to sympathetic and parasympathetic preganglionic neurons. *Journal of the autonomic nervous system , 3*, 265-275.

Logothetis, N. (2002). The neural basis of the blood-oxygen-level-dependent functional magnetic resonance imaging signal. *Philosophical Transactions of the Royal Society of London , 357*, 1003-1037.

Macefield, V., Gandevia, S., & Henderson, L. (2006). Neural sites involved in the sustained increase in muscle sympathetic activity induced by inspiratory capacity apnea: a fMRI study. *Journal of Applied Physiology , 100*, 266-273.

Macey, P., Wu, P., Kumar, R., Ogren, J., Richardson, H., Woo, M., et al. (2012). Differential responses of the insular cortex gyri to autonomic challenges. *Autonomic Neuroscience: Basic and Clinical , 168*, 72-81.

Maciel, B., Gallo Jr., L., JA, M. N., & Martins, L. (1987). Autonomic nervous control of the heart rate during isometric exercise in normal man. *European Journal of Physiology , 408*, 173-177.

Malik, M., Camm, A., & members of the Task Force of the European Society of Cardiology. (1996). Heart Rate Variability: standards of measurements, physiological interpretation and clinical use. *Circulation , 93* (5), 1043-1065.

Mark, A., Victor, R., Nerhed, C., & Gunnar Wallin, B. (1985). Microneurographic studies of the mechanisms of sympathetic nerve responses to static exercise in humans. *Circulatory Research , 57* (3), 461-469.

Matthews, S., Paulus, M., Simmons, A., Nelesen, R., & Dimsdale, J. (2004). Functional subdivisions within anterior cingulate cortex and their relationship to autonomic nervous system function. *NeuroImage , 22*, 1151-1156.

McCloskey, D., & Mitchell, J. (1972). Reflex cardiovascular and respiratory responses originating in exercising muscle. *Journal of Physiology , 224*, 173-186.

Melzack R, W. P. (1965). Pain mechanisms: a new theory. *Science , 150*, 971-979.

Moayedi, M., & Davis, K. (2013). Theories of pain: from specificity to gate control. *Journal of Neurophysiology , 109*, 5-12.

Napadow, V., Dhond, R., Conti, G., Makris, N., Brown, E., & Barbieri, R. (2008). Brain correlates of autonomic modulation: Combining heart rate variability with fMRI. *NeuroImage , 42*, 169-177.

Naver, H., Blomstrand, C., & Wallin, B. (1996). Reduced heart rate variability after right-sided stroke. *Stroke , 27* (2), 247-251.

Norris, D. (2006). Principles of magnetic resonance assessment of brain function. *Journal of magnetic resonance imaging , 23*, 794-807.

Okutucu, S., Karakulak, U., Aytemir, K., & Oto, A. (2011). Heart rate recovery: a practical and clinical indicator of abnormal cardiac autonomic function. *Expert Review of Cardiovascular Therapy , 9* (11), 1417-1430.

Ongur, D., & Price, J. (2000). The organization of the networks within the orbital and medial prefrontal cortex of rats, monkeys and humans. *Cerebral Cortex , 10* (3), 206-219.

Ongur, D., An, X., & Price, J. (1998). Prefrontal cortical projections to the hypothalamus in macaque monkeys. *The Journal of Comparative Neurology , 401*, 480-505.

Oldfield, RC. (1971). The assessment and analysis of handedness: Edinburgh inventory. *Neuropsychologia, 9*, 97-113.

Oppenheimer, S., & Cechetto, D. (1990). Cardiac chronotopic organization of the rat insular cortex. *Brain Research , 533*, 66-72.

Oppenheimer, S., Gelb, A., Girvin, J., & Hachinski, V. (1991). Cardiovascular effects of human insular cortex stimulation. *Neurology , 42*, 1727-1732.

Oppenheimer, S., Kedem, G., & Martin, W. (1996). Left-insular cortex lesions perturb cardiac autonomic tone in humans. *Clinical Autonomic Research , 6*, 131-140.

Owens NC and Verberne, A. (2001). Regional haemodynamic responses to activation of prefrontal cortex depressor regions. *Brain Research , 919*, 221-231.

Owens, N., & Verberne, A. (1996). An electrophysiological study of the medial prefrontal cortical projection to the nucleus of the solitary tract in the rat. *Experimental Brain Research , 110*, 55-61.

Owens, N., & Verberne, A. (2001). Regional haemodynamica responses to activation of the medial prefrontal cortex depressor region. *Brain Research , 919*, 221-231.

Owens, S., Atkinson, E., & Lees, D. (1979). Thermographic evidence of reduced sympathetic tone with transcutaneous nerve stimulation. *Anesthesiology , 50*, 62-65.

Pagani, M., Lombardi, F., Guzzetti, S., Rimoldi, O., Furlan, R., Pizzinelli, P., et al. (1986). Power spectral analysis of heart rate and arterial pressure variabilities as a marker of sympatho-vagal interaction in man and conscious dog. *Circulation Research , 59*, 178-193.

Petro, J., Hollander, A., & Bouman, L. (1970). Instantaneous cardiac acceleration in man induced by a voluntary muscle contraction. *Journal of Applied Physiology , 29* (6), 794-798.

Pomeranz, B., Macaulay, R., Caudill, M., Kutz, I., Adam, D., Gordon, D., et al. (1985). Assessment of autonomic function in humans by heart rate spectral analysis. *American Journal of Physiology - heart and Circulatory Physiology , 248*, H151-H153.

Pott, L., & Pusch, H. (1979). A kinetic model for the muscarinic action of acetylcholine. *Pflugers Archiv European Journal of Physiology , 383*, 75-77.

Raichle, M., MacLeod, A., Snyder, A., Powers, W., Gusnard, D., & Shulman, G. (2001). A default mode of brain function. *Proceedings of the National Academy of Science , 98* (2), 676-682.

Rolls, E., Inoue, K., & Browning, A. (2003). Activity of primate subgenual cingulate cortex neurons is related to sleep. *Journal of Neurophysiology , 90*, 134-142.

Samar, V., Bopardikar, A., Rao, R., & Swartz, K. (1999). Wavelet analysis of neuroelectric waveforms: a conceptual tutorial. *Brain and Language , 66*, 7-60.

Sanderson, J., Tomlinson, B., Lau, M., So, K., Cheung, A., Critchley, J., et al. (1995). The effect of transcutaneous electrical nerve stimulation (TENS) on autonomic cardiovascular reflexes. *Clinical Autonomic Research , 5*, 81-84.

Saper, C. (1982). Reciprocal parabrachial-cortical connections in the rat. *Brain Research , 242*, 33-40.

Schneider, R., Friedman, D., & Mishkin, M. (1993). A modality-specific somatosensory area within the insula of the rhesus monkey. *Brain Research , 621*, 116-120.

Shields, R. J. (1993). Functional anatomy of the autonomic nervous system. *Journal of Clinical Neurophysiology , 10* (1), 2-13.

Shipley, M. (1982). Insular cortex projections to the nucleus of the solitary tract and the brainstem visceromotor regions in the mouse. *Brain Research Bulletin , 8*, 139-148.

Shipley, M., & Sanders, M. (1982). Special senses are really special: Evidence for a reciprocal, bilateral pathway between insular cortex and nucleus parabrachialis. *Brain Research Bulletin , 8*, 493-501.

Shoukas, A., & Sagawa, K. (1973). Control of total vascular capacity by the carotid sinus baroreceptor reflex. *Circulation Research , 33*, 22-33.

Swett, J., & Bourassa, C. (1981). Electrical stimluation of peripheral nerve. In M. Patterson, & R. Kesner (Eds.), *Electrical Stimulation Research Techniques* (Vol. 3, pp. 244-284). New York: Academic Press.

Terreberry, R., & Neafsey, E. (1983). Rat medial frontal cortex: a visceral motor regions with a direct projection to the solitary nucleus. *Brain Research , 278*, 245-249.

Thirion, B., Pinel, P., Meriaux, S., Roche, A., Dehaene, S., & Poline, J. (2007). Analysis of a large fMRI cohort: Statistical and methodological issues for group analyses. *NeuroImage , 35*, 105-120.

Toda, N., & Shimamoto, K. (1968). The influence of sympathetic stimulation on transmembrane potentials in the S-A node. *The Journal of Pharmacology and Experimental Therapeutics , 159* (2), 298-305.

Toledo, E., Gurevitz, O., Hod, H., Eldar, M., & Akselrod, S. (2003). Wavelet analysis of instantaneous heart rate: a study of autonomic control during thrombolysis. *American Journal of Physiology - Regulatory, Integrative and Comparative Physiology , 284*, R1079-R1091.

Torrence, C., & Compo, G. (1998). A practical guide to wavelet analysis. *Bulletin of the American Meterological Society , 79* (1), 61-78.

Van De Borne, P., Montano, N., Narkiewicz, K., Degaute, J., Malliani, A., Pagani, M., et al. (2001). Importance of ventilation in modulating interaction between sympathetic drive and cardiovascular variability. *American Journal of Physiology - Heart and Circulatory Physiology , 280*, H722-H729.

van Ravenswaaij-Arts, C., Kollee, L., Hopman, J., Stoelinga, G., & van Geijn, H. (1993). Heart rate variability. *Annals of Internal Medicine , 118*, 436-447.

Verberne, A. (1996). Medullary sympathoexcitatory neurons are inhibited by activation of the medial prefrontal cortex in the rat. *American Journal of Physiology - Regulatory, Integrative and Comparative Physiology , 270*, R713-R719.

Verberne, A., & Owens, N. (1998). Cortical modulation of the cardiovascular system. *Progress in Neurobiology , 54* (2), 149-168.

Williamson, J., Nobrega, A., McColl, R., Mathews, D., Winchester, P., Friberg, L., et al. (1997). Activation of the insular cortex during dynamic exercise in humans. *Journal of Physiology , 503*, 277-283.

Wong, S., Masse, N., Kimmerly, D., Menon, R., & Shoemaker, J. (2007b). Ventral medial prefrontal cortex and cardiovagal control on conscious humans. *Neuoimaging , 35* (2), 698-708.

Yasuma, F., & Hayano, J. (2004). Respiratory Sinus Arrhythmia. *CHEST Journal , 125* (2), 683-690.

Zhang, Z., & Oppenheimer, S. (2000). Baroreceptive and somatosensory convergent thalamic neurons project to the posterior insula cortex in the rat. *Brain Research , 861*, 241-256.

Zhang, Z., Dougherty, P., & Oppenheimer, S. (1998). Characterization of baroreceptor-related neurons in the monkey insular cortex. *Brain Research* , 303-306.

Zhang, Z., Dougherty, P., & Oppenheimer, S. (1999). Monkey insular cortex neurons response to baroreceptive and somatosensory convergent inputs. *Neuorscience , 94* (2), 351-360.

Ziegler, G., Dahnke, R., Yeragani, V., & Bar, K. (2009). The relation of ventromedial prefrontal cortex activity and heart rate fluctuations at rest. *European Journal of Neuroscience , 30*, 2205-2210.

APPENDICES

APPENDIX A – Supplementary Heart Rate Variability Data

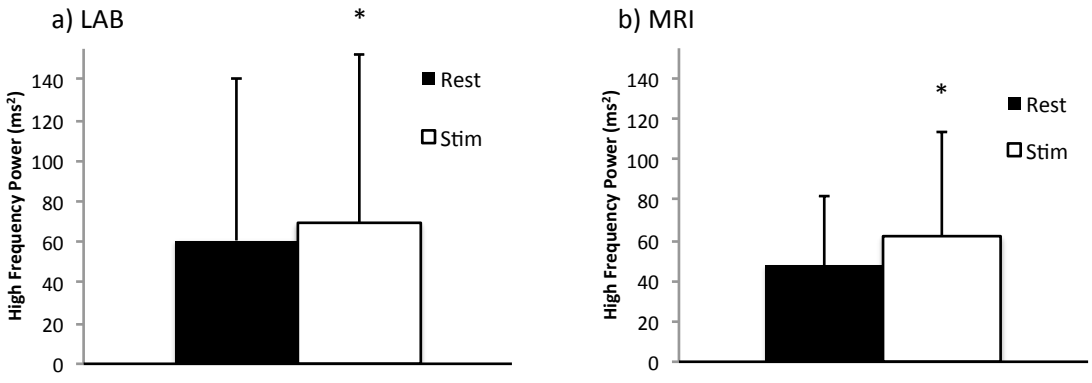

Figure A. 1: High frequency HRV (non-normalized units) during rest and STIM during a) LAB and b) MRI recording sessions. *p<0.01.

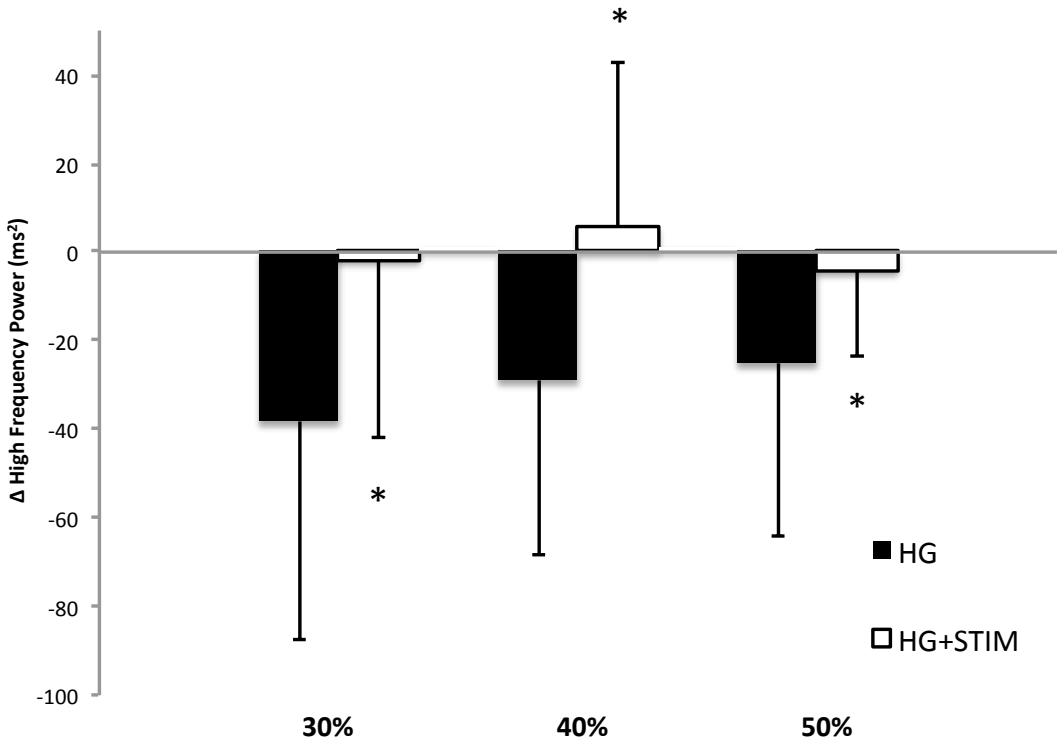

Figure A. 2: Change in high frequency HRV (non-normalized units) during HG and HG+STIM at 30, 40, 50% MVC during LAB visit. *p<0.05. HRV, heart rate variability; HG, handgrip; HG+STIM, handgrip+sub-motor somatosensory stimulation.

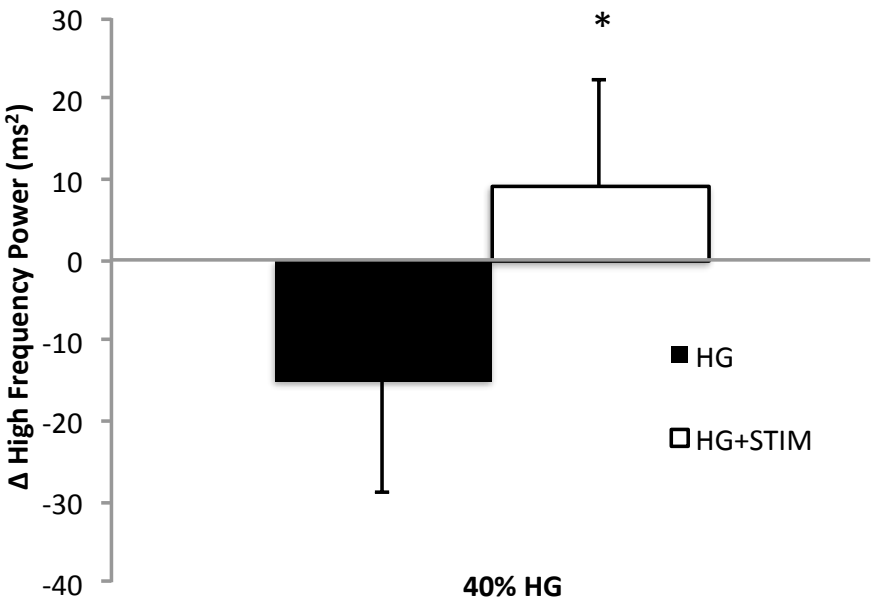

Figure A. 3: Change in high frequency HRV (non-normalized units) during HG and HG+STIM at 40% MVC during the MRI visit. *p<0.05. HRV, heart rate variability; HG, handgrip; HG+STIM, handgrip+sub-motor somatosensory stimulation.

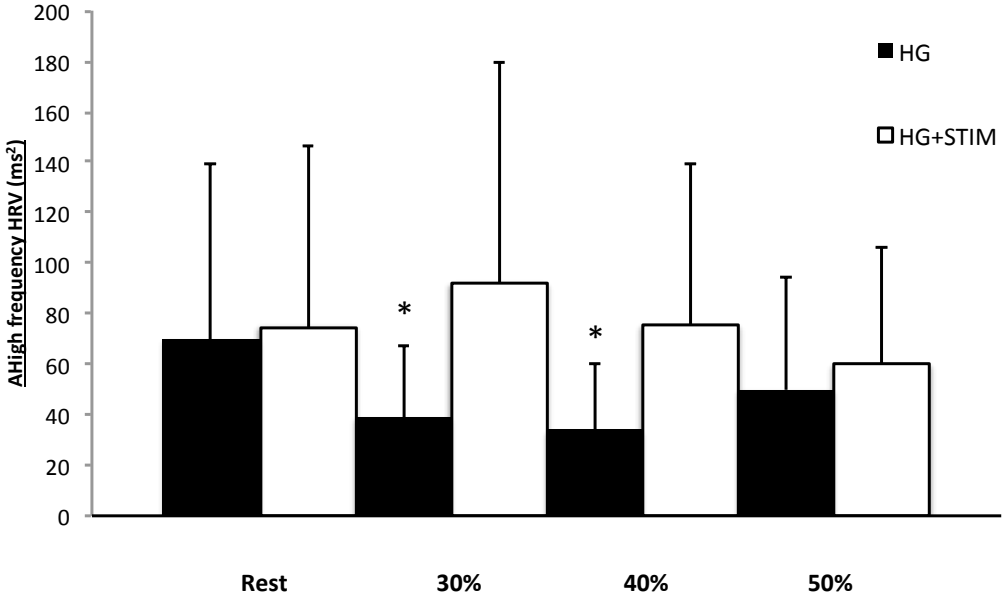

Figure A. 4: High frequency HRV (non-normalized units) at rest, 30, 40 and 50% HG and HG+STIM. *p<0.01 different from rest. HRV, heart rate variability; HG, handgrip; HG+STIM, handgrip+sub-motor somatosensory stimulation.

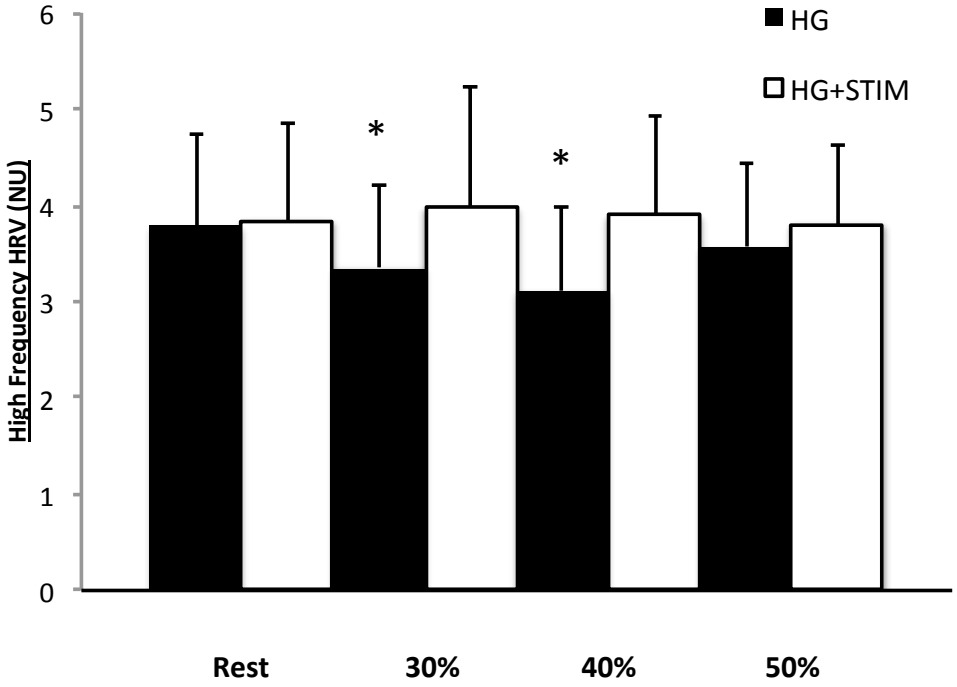

Figure A. 5: High frequency HRV (normalized unit) at rest, 30, 40, and 50% HG and HG+STIM. *p<0.01 different from rest. HRV, heart rate variability; HG, handgrip; HG+STIM, handgrip+sub-motor somatosensory stimulation.

APPENDIX B – Ethics Approval

Research Western

Use of Human Participants - Ethics Approval Notice

Principal Investigator: Dr. Kevin Shoemaker
Review Number: 17810
Review Level: Delegated
Approved Local Adult Participants: 200
Approved Local Minor Participants: 0
Protocol Title: Architecture of Cortical Somatosensory and Autonomic Neural Networks Supporting Muscular Movement: Impacts of Vascular Disease and Exercise Interventions.
Department & Institution: Kinesiology, University of Western Ontario
Sponsor: Canadian Institutes of Health Research

Ethics Approval Date: August 12, 2011 **Expiry Date:** December 31, 2016
Documents Reviewed & Approved & Documents Received for Information:

Document Name	Comments	Version Date
Revised Letter of Information & Consent		
Other	Revised recruitment letter	

This is to notify you that The University of Western Ontario Research Ethics Board for Health Sciences Research Involving Human Subjects (HSREB) which is organized and operates according to the Tri-Council Policy Statement: Ethical Conduct of Research Involving Humans and the Health Canada/ICH Good Clinical Practice Practices: Consolidated Guidelines; and the applicable laws and regulations of Ontario has reviewed and granted approval to the above referenced revision(s) or amendment(s) on the approval date noted above. The membership of this REB also complies with the membership requirements for REB's as defined in Division 5 of the Food and Drug Regulations.

The ethics approval for this study shall remain valid until the expiry date noted above assuming timely and acceptable responses to the HSREB's periodic requests for surveillance and monitoring information. If you require an updated approval notice prior to that time you must request it using the UWO Updated Approval Request Form.

Members of the HSREB who are named as investigators in research studies, or declare a conflict of interest, do not participate in discussion related to, nor vote on, such studies when they are presented to the HSREB.

The Chair of the HSREB is Dr. Joseph Gilbert. The UWO HSREB is registered with the U.S. Department of Health & Human Services under the IRB registration number IRB 00000940.

APPENDIX C – Figure Republication Permissions

JOHN WILEY AND SONS LICENSE TERMS AND CONDITIONS

May 28, 2013

This is a License Agreement between Jacquie Baker ("You") and John Wiley and Sons ("John Wiley and Sons") provided by Copyright Clearance Center ("CCC"). The license consists of your order details, the terms and conditions provided by John Wiley and Sons, and the payment terms and conditions.

All payments must be made in full to CCC. For payment instructions, please see information listed at the bottom of this form.

License Number	3157730790730
License date	May 28, 2013
Licensed content publisher	John Wiley and Sons
Licensed content publication	Journal of Magnetic Resonance Imaging
Licensed content title	Principles of magnetic resonance assessment of brain function
Licensed copyright line	Copyright © 2006 Wiley-Liss, Inc.
Licensed content author	David G. Norris
Licensed content date	Apr 28, 2006
Start page	794
End page	807
Type of use	Dissertation/Thesis
Requestor type	University/Academic
Format	Print and electronic
Portion	Figure/table
Number of figures/tables	1
Original Wiley figure/table number(s)	Figure 1
Will you be translating?	No
Total	0.00 USD
Terms and Conditions	

TERMS AND CONDITIONS

This copyrighted material is owned by or exclusively licensed to John Wiley & Sons, Inc. or one of its group companies (each a "Wiley Company") or a society for whom a Wiley Company has exclusive publishing rights in relation to a particular journal (collectively "WILEY"). By clicking "accept" in connection with completing this licensing transaction,

ACP
American College of Physicians
internal medicine | *Doctors for Adults*

WAA1318158

June 18, 2013

Dear:

Thank you for your request for print (dissertation) format of the following from *Annals of Internal Medicine:*

Figure 2: Conny M. A. van Ravenswaaij-Arts, MD, et al, Heart Rate Variability. Annals of Internal Medicine, Mar 15, 1993 118

Permission is granted to print the preceding material with the understanding that you will give appropriate credit to *Annals of Internal Medicine* as the original source of the material. Any translated version must carry a disclaimer stating that the American College of Physicians is not responsible for the accuracy of the translation. This permission grants non-exclusive, worldwide rights for this edition in print (dissertation) format for not for only. ACP does not grant permission to reproduce entire articles or chapters on the Internet unless explicit permission is given. This letter represents the agreement between ACP and Jacquie Baker for request WAA13181 and supersedes all prior terms from the requestor. The Annals of Internal Medicine wants to encourage users to go to the original article on the website for scientific integrity, in the event there are retractions and corrections.

CURRICULUM VITAE

Jacquie Baker

Post-Secondary Education and Degrees:	The University of Western Ontario London, Ontario, Canada Honors Specialization Bachelor of Science, Kinesiology	2006-2010
	The University of Western Ontario London, Ontario, Canada Master of Science, Integrative Exercise Physiology	2011-2013
Honors and Awards:	Western Graduate Research Scholarship	2011-2012 2012-2013
Work Experience:	Graduate Teaching Assistant	2011-2012 2012-2013
Conference Abstracts:	**Baker, JR**. and Shoemaker, J.K. (2013). Effect of isometric handgrip exercise on heart rate variability with and without somatosensory stimulation.	
	Lalande, S., Sawicki, CP., **Baker, JR**., and Shoemaker, J.K. (2012). Effect of aging on the hemodynamic and sympathetic response at the onset of isometric handgrip exercise.	
In preparation:	Lalande, S., Sawicki, CP., **Baker, JR**., and Shoemaker, J.K. (2012). Effect of aging on the hemodynamic and sympathetic response at the onset of isometric handgrip exercise.	